

# Model-Free Practical Cooperative Control for Diffusively Coupled Systems via Passivity Theory and Network Optimization

Miel Sharf, Anne Romer, Daniel Zelazo and Frank Allgöwer

**Abstract**—In this paper, we develop a data-based controller design framework for diffusively coupled systems with guaranteed convergence to an  $\epsilon$ -neighborhood of the desired formation. The controller is comprised of a fixed controller with an adjustable gain on each edge. Via passivity theory and network optimization we not only prove that there exists a gain to attain the desired formation control goal, but we present a data-based method to find an upper bound on this gain. Furthermore, by allowing for additional experiments, the conservatism of the upper bound can be reduced via iterative sampling schemes. The introduced scheme is based on the assumption of passive systems, which we relax by discussing different methods for estimating the systems' passivity shortage, as well as applying transformations passivizing them. Finally, we illustrate the developed model-free cooperative control scheme with two case studies.

## I. INTRODUCTION

Multi-agent systems have received extensive attention in the past years, due to their appearance in many fields of engineering, exact sciences and social sciences. Examples include robotics [1], [2], neural networks [3], [4], traffic engineering [5], gene regulation [6], [7], physics [8], ecology [9], [10], and even data mining [11], behavioural sciences [12] and finance [13], [14]. The state-of-the-art approach to model-based control for multi-agent systems offers rigorous stability analysis, performance guarantees and systematic insights into the considered problem. However, with the growing complexity of systems, the modeling process is reaching its limits. Obtaining a reliable mathematical model of the agents becomes a time-intensive and almost impossible task.

At the same time, modern technology allows for gathering and storing more and more data from systems and processes. Therefore, there has been an increasing interest in what is called *data-driven controller design*. There have been different approaches to data-driven controller design very generally (see, e.g., [15], [16]), and some approaches to multi-agent control from data more particularly [17]–[19]. Nonetheless, the centralized nature of the general design schemes, or the specificity of the agents' model and high measurement rate for the multi-agent approaches, prevents the application of many of the aforementioned approaches in various real-world scenarios.

M. Sharf and D. Zelazo are with the Faculty of Aerospace Engineering, Israel Institute of Technology, Haifa, Israel. A. Romer and F. Allgöwer are with the Institute for Systems Theory and Automatic Control, University of Stuttgart, Germany. msharf@tx.technion.ac.il, anne.romer@ist.uni-stuttgart.de. This work was supported by the German-Israeli Foundation for Scientific Research and Development.

In this work, we develop a data-driven controller approach for multi-agent systems that comes with rigorous theoretical analysis and stability guarantees for the closed loop, with almost no assumptions on the agents and very few measurements needed. The approach is based on the notion of high-gain controllers. Some ideas on high-gain approaches to cooperative control can be found in [20] and references therein. In [21], the authors provide a high-gain condition in the design of distributed  $H_\infty$  controllers for platoons with undirected topologies, while there are also many approaches to (adaptively) tuning the coupling weights, e.g. [22]. Our approach provides an upper bound on a high-gain controller on the basis of passivity measures. Passivity properties of the components can provide sufficient abstractions of their detailed dynamical models for guaranteed control. Such passivity properties, in turn, can be obtained from data as ongoing work shows (e.g., [23]–[26]).

Passivity is a well-known tool for controller synthesis [27], [28], which is useful, beyond convergence analysis, for its powerful properties such as compositionality. It was first introduced in the field of multi-agent systems in the seminal works of Arcak [29], [30], and was since explored in many variants in the context of multi-agent systems in many other works [2], [31]–[38]. We focus on the variant known as maximal equilibrium independent passivity (MEIP), as presented in [33].

This work generally studies the problem of controller synthesis for diffusively coupled systems. The control objective is to converge to an  $\epsilon$ -neighborhood of a constant prescribed relative output vector. That is, for some tolerance  $\epsilon > 0$ , we aim to design controllers so that the steady-state relative output limit is  $\epsilon$ -close to the prescribed values. The related problem of practical synchronization of multi-agent systems have been considered in [39], in which the plants were assumed to be known up to some bounded additive disturbance. However, a nominal model of the plant was needed to achieve the practical synchronization. It was also pursued in [40], in which strong coupling was used to drive agents to a neighborhood of a common trajectory, but again, a model for the agents was needed.

Our contributions are as follows. We present a model-free data-driven method for solving the practical formation control problem. This is done by cascading a fixed controller and an adjustable gain on each edge. We show how this gain can be chosen to guarantee a practical solution to the control goal for the closed loop. Furthermore, we provide

schemes to compute this gain offline only from input-output data without any model of the agents. In fact, this gain can be computed from only three experiments (per agent) and can be improved (i.e., rendered less conservative) with further data samples. If iterative experiments can be performed, we also provide an approach for applying different gains over different edges to further reduce any conservatism. We survey the different advantages for each of the methods and discuss their applicability in terms of the number of required measurements, or trade-offs in terms of the norm of the adjustable gain vector. We also provide simulations presenting the effectiveness of the presented model-free controller synthesis methods.

*Notations:* We employ basic notions from algebraic graph theory throughout the paper [41]. An undirected graph  $\mathcal{G} = (\mathbb{V}, \mathbb{E})$  consists of finite sets of vertices  $\mathbb{V}$  and edges  $\mathbb{E} \subset \mathbb{V} \times \mathbb{V}$ . We denote the edge having ends  $i$  and  $j$  in  $\mathbb{V}$  by  $k = \{i, j\} \in \mathbb{E}$ . For each edge  $k$ , we pick an arbitrary orientation and denote  $k = (i, j)$  when  $i \in \mathbb{V}$  is the *head* of edge  $k$  and  $j \in \mathbb{V}$  the *tail*. The incidence matrix of  $\mathcal{G}$ , denoted  $\mathcal{E} \in \mathbb{R}^{|\mathbb{E}| \times |\mathbb{V}|}$ , is defined such that for an edge  $k = (i, j) \in \mathbb{E}$ , we have  $[\mathcal{E}]_{ik} = +1$ ,  $[\mathcal{E}]_{jk} = -1$ , and  $[\mathcal{E}]_{\ell k} = 0$  for  $\ell \neq i, j$ . The diameter of the graph  $\mathcal{G}$  is denoted by  $\text{diam}(\mathcal{G})$ .

Furthermore, we'll use some notions from linear algebra. For every vector  $v \in \mathbb{R}^n$ ,  $\text{diag}(v)$  denotes the  $n \times n$  diagonal matrix with the entries of  $v$  on its diagonal. The image of any linear map  $T$  between vector spaces will be denoted by  $\text{Im}(T)$ . Moreover, given a vector space  $V$  and a subspace  $W$ , we'll denote the linear map of orthogonal projection on  $W$  by  $\text{Proj}_W$ . Also, for two sets  $A, B \subseteq \mathbb{R}^d$ , we define  $A + B = \{a + b : a \in A, b \in B\}$ . Furthermore,  $\|\cdot\|$  is the Euclidean norm.

Lastly, if  $\Sigma$  is a dynamical system with input  $u$  and output  $y$ , and  $M$  is a linear map of appropriate dimension, we can consider the cascaded system of  $\Sigma$  and  $M$ . The cascade of  $\Sigma$  after  $M$  is denoted  $\Sigma M$ , and the cascade of  $\Sigma$  before  $M$  is denoted  $M\Sigma$ .

## II. BACKGROUND: NETWORK OPTIMIZATION AND PASSIVITY IN COOPERATIVE CONTROL

Our goal in this subsection is to describe the diffusive coupling networks studied in [33], and to present the passivity-based network optimization framework achieved for multi-agent systems. See also [34], [35].

### A. Diffusively Coupled Systems and Steady-State Relations

Diffusively coupled networks are composed of SISO agents interacting over a graph  $\mathcal{G} = (\mathbb{V}, \mathbb{E})$ . Each vertex  $i \in \mathbb{V}$  represents an agent, modeled as a SISO dynamical system

$$\Sigma_i : \begin{cases} \dot{x}_i = f_i(x_i, u_i) \\ y_i = h_i(x_i, u_i), \end{cases} \quad (1)$$

with state  $x_i$ , input  $u_i$  and output  $y_i$ . Furthermore, each edge  $e \in \mathbb{E}$  represents a SISO dynamical system (a SISO controller) of the form

$$\Pi_e : \begin{cases} \dot{\eta}_e = \phi_e(\eta_e, \zeta_e) \\ \mu_e = \psi_e(\eta_e, \zeta_e), \end{cases} \quad (2)$$

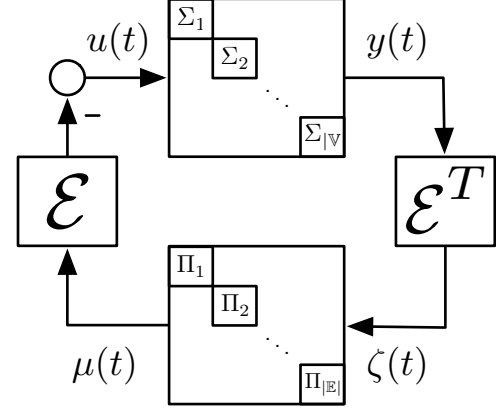


Fig. 1. Block-diagram of the diffusively-coupled network  $(\Sigma, \Pi, \mathcal{G})$ .

with state  $\eta_e$ , input  $\zeta_e$  and output  $\mu_e$ . To understand how these systems are connected to each other, we consider the stacked inputs and outputs of the agents and controllers as  $y = [y_1, \dots, y_{|\mathbb{V}|}]^T$ ,  $u = [u_1, \dots, u_{|\mathbb{V}|}]^T$ ,  $\zeta = [\zeta_1, \dots, \zeta_{|\mathbb{E}|}]^T$  and  $\mu = [\mu_1, \dots, \mu_{|\mathbb{E}|}]^T$ . The system is connected via the relations  $\zeta = \mathcal{E}^T y$  and  $u = -\mathcal{E} \mu$ , where  $\mathcal{E}$  is the incidence matrix of the graph  $\mathcal{G}$ . In other words, if we stack all agents together to get a stacked dynamical system  $\Sigma$ , and stack all controllers together to get a stacked dynamical system  $\Pi$ , then the closed-loop is just the feedback connection of the systems  $\Sigma$  and  $\mathcal{E}\Pi\mathcal{E}^T$ . See Fig. 1 for an illustration of this closed-loop diffusively coupled network, which we will denote by the triplet  $(\mathcal{G}, \Sigma, \Pi)$ .

We will be interested in steady-states of the closed-loop system. It's clear that if the stacked vectors  $(u, y, \zeta, \mu)$  are a steady-state for  $(\mathcal{G}, \Sigma, \Pi)$ , then for every vertex  $i \in \mathbb{V}$ ,  $(u_i, y_i)$  is a steady-state input-output pair for the system  $\Sigma_i$ , and for every edge  $e \in \mathbb{E}$ ,  $(\zeta_e, \mu_e)$  is a steady-state input-output pair for the system  $\Pi_e$ . This motivates the exploration of *steady-state input-output relations*, first defined in [33].

**Definition 1.** *The steady-state relation of a dynamical system is a set containing all the steady-state input-output pairs of the system.*

We will denote the steady-states relations of  $\Sigma_i$ ,  $\Pi_e$ ,  $\Sigma$ , and  $\Pi$  as  $k_i$ ,  $\gamma_e$ ,  $k$ , and  $\gamma$ , accordingly.

**Remark 1.** *We will sometimes abuse the notation and consider this relation as a set-valued map. Indeed, for any input  $u$  we can define the set  $k(u)$  by*

$$k(u) = \{y : (u, y) \in k\},$$

*and similarly for  $k_i$ ,  $\gamma_e$ , and  $\gamma$ . Also, we can consider the inverse relation  $k^{-1}$  as the set-valued map assigning the following set to a steady-state output  $y$ ,*

$$k^{-1}(y) = \{u : y \in k(u)\},$$

*i.e., the set of all steady-state inputs corresponding to the steady-state output  $y$ . We define this similarly for  $k_i$ ,  $\gamma_e$ , and  $\gamma$ .*

With this definition,  $(u, y, \zeta, \mu)$  is a steady-state of  $(\mathcal{G}, \Sigma, \Pi)$  if and only if  $y \in k(u)$ ,  $\mu \in \gamma(\zeta)$ ,  $\zeta = \mathcal{E}^T y$  and  $u = -\mathcal{E}\mu$ . Equivalently, if the zero vector 0 lies in the set  $k^{-1}(y) + \mathcal{E}\gamma(\mathcal{E}^T y)$  then  $y$  is a steady-state output for  $(\mathcal{G}, \Sigma, \Pi)$  [33], [34].

### B. Maximum Equilibrium-Independent Passivity and the Network Optimization Framework

One of the main concepts allowing us to connect multi-agent systems to the network optimization world is the concept of monotone relations.

**Definition 2.** A steady-state relation is monotone if for any two points  $(u_1, y_1)$  and  $(u_2, y_2)$  in the relation,  $u_1 < u_2$  implies  $y_1 \leq y_2$ . We say that a monotone relation is maximally monotone if it is not contained in a larger monotone relation.

In order to connect this definition to the system-theoretic world, we define the notion of maximum equilibrium-independent passivity.

**Definition 3** ([33]). A SISO system is said to be (output-strictly) maximum equilibrium-independent passive (MEIP) if the following two conditions hold:

- i) The system is (output-strictly) passive with respect to any steady-state input-output pair it has, and
- ii) it's steady-state input-output relation is maximally monotone.

One important property of maximally monotone relations is that they are subgradients of convex functions [42]. In this direction, we assume that the agents and controllers of the diffusively-coupled network  $(\mathcal{G}, \Sigma, \Pi)$  are MEIP. Let  $K_i$ , and  $\Gamma_e$  be the corresponding convex integral functions for the steady-state relations  $k_i, \gamma_e$ . In other words,  $\partial K_i = k_i$  and  $\partial \Gamma_e = \gamma_e$ , where  $\partial$  denotes the subdifferential of convex functions [42]. We shall denote  $K = \sum_{i \in \mathcal{V}} K_i$  and  $\Gamma = \sum_{e \in \mathcal{E}} \Gamma_e$ , so that  $\partial K = k$  and  $\partial \Gamma = \gamma$ . One can consider the dual functions of the convex functions  $K_i, \Gamma_e, K, \Gamma$  are defined using the Legendre transform,  $K^*(y) = \sup_u \{u^T y - K(u)\} = -\inf_u \{K(u) - u^T y\}$ , and similarly for  $K_i^*, \Gamma_e^*$  and  $\Gamma^*$ . The main property of these dual function is that  $\partial K^* = k^{-1}$ ,  $\partial \Gamma^* = \gamma^{-1}$ ,  $\partial K_i^* = k_i^{-1}$  and  $\partial \Gamma_e^* = \gamma_e^{-1}$  [42].

Now, we resume our interest in steady-states for the diffusively coupled network  $(\mathcal{G}, \Sigma, \Pi)$ . We recall that a constant signal  $y$  was the steady-state output of the diffusively coupled network if and only if  $0 \in k^{-1}(y) + \mathcal{E}\gamma(\mathcal{E}^T y)$ . Restating this result in the language of convex functions gives the following theorem.

**Theorem 1** ([33]). Consider the diffusively coupled network  $(\mathcal{G}, \Sigma, \Pi)$ . Assume all agents  $\Sigma_i$  are MEIP, and all controllers  $\Pi_e$  are output-strictly MEIP (or vice versa). Denote the steady-state relations of  $\Sigma_i, \Pi_e, \Sigma$  and  $\Pi$  as  $k_i, \gamma_e, k$  and  $\gamma$  accordingly, and let  $K_i, \Gamma_e, K, \Gamma$  be the corresponding convex integral functions. Then the closed-loop system converges to a steady-state  $(u, y, \zeta, \mu)$ , such that  $(y, \zeta)$  and  $(u, \mu)$  are a pair of dual solutions to the following convex optimization problems:

Optimal Potential Problem		Optimal Flow Problem	
$\min_{y, \zeta}$	$K^*(y) + \Gamma(\zeta)$	$\min_{u, \mu}$	$K(u) + \Gamma^*(\mu)$
s.t.	$\mathcal{E}^T y = \zeta$	s.t.	$\mu = -\mathcal{E}u$

The two network optimization problems above will be denoted often by (OPP) and (OFP) respectively. These problems are two fundamental problem in the field of network optimization, which deals with optimization problems defined on graphs [42]. The names “optimal potential problem” and “optimal flow problem” are inspired from standard nomenclature in this field.

### III. PROBLEM FORMULATION

We focus on relative-output based formation control. In this problem, the agents know the relative output  $\zeta_e = y_i - y_j$  with respect to their neighbors, and the control goal is to converge to a steady-state with prescribed relative outputs  $\zeta_e = y_i - y_j$ . Examples include the consensus problem, in which all outputs must agree, as well as relative-position based formation control of robots, in which the robots are required to organize themselves in a desired spatial structure [43].

More specifically, we are given a graph  $\mathcal{G}$  and agents  $\Sigma$ , and our goal is to design controllers  $\Pi$  so that the formation vector  $\zeta(t)$  of the diffusively coupled network  $(\mathcal{G}, \Sigma, \Pi)$  will converge to a desired, given steady-state vector  $\zeta^*$ . One evident solution to the problem is to apply a (shifted) integrator as a controller. However, this solution will not always work even when the agents are MEIP.

**Example 1.** Consider the case of agents  $\Sigma_i$  with integrator dynamics, together with the controllers  $\Pi_e$  according to the previous idea, where we desire consensus (i.e.,  $\zeta^* = 0$ ) over a connected graph  $\mathcal{G}$ ,

$$\Sigma_i : \begin{cases} \dot{x}_i = u_i \\ y_i = x_i \end{cases}, \quad \Pi_e : \begin{cases} \dot{\eta}_e = \zeta_e \\ \mu_e = \eta_e \end{cases}.$$

The trajectories of the diffusively-coupled system can be understood by noting that the closed-loop system yields the second-order dynamics  $\ddot{x} = -\mathcal{E}\mathcal{E}^T x$ . Decomposing  $x$  using a basis of eigenvectors of the graph Laplacian  $\mathcal{E}\mathcal{E}^T$ , which is a positive semi-definite matrix, we see that the trajectory of  $x(t)$  oscillates around the consensus manifold  $\{x : \exists \lambda \in \mathbb{R} \ x = \lambda \mathbf{1}_n\}$ . Specifically,  $x(t) - \frac{1}{n} \mathbf{1}_n^T x(t) = \sum_{i=2}^n c_i \cos(\sqrt{\lambda_i} t + \varphi_i) v_i$ , where  $\lambda_2, \dots, \lambda_n > 0$  are the non-trivial eigenvalues of the graph Laplacian,  $v_2, \dots, v_n$  are corresponding unit-length eigenvectors, and  $c_i, \varphi_i$  are constants depending on the initial conditions  $x(0), \eta(0)$ . Thus  $x(t) = y(t)$  does not converge anywhere, let alone to consensus. Moreover, the vector  $\zeta(t) = \mathcal{E}^T y(t) = \sum_{i=2}^n \lambda_i c_i \cos(\sqrt{\lambda_i} t + \varphi_i) v_i$  does not converge as  $t \rightarrow \infty$ . Thus the integrator controller does not solve the position-based formation control problem in this case.

Even if the integrator would solve this problem in general, we would like more freedom in choosing the controller. In practice, one might want to design the controller to satisfy extra requirements (like  $\mathcal{H}_2$ - or  $\mathcal{H}_\infty$ -norm minimization, or making sure that certain restrictions on the behavior of the system are not broken). We do not try and satisfy these more

complex requirements, but instead show that a large class of controllers can be used to solve the practical formation control problem. In turn, this allows one to choose from a wide range of controllers, and try and satisfy additional desired properties. In [34], there is an algorithm solving the relative position-based formation control problem with ease, as long as the agents are MEIP and a perfect model of each agent is known. This algorithm allows a vast amount of freedom in the choice of controllers. However, in practice we oftentimes have no exact model of our agents, or there is even no closed form mathematical model available at all.

To formalize the goals we aim at, we define the notion of *practical formation control*.

**Problem 1.** *Given a graph  $\mathcal{G}$ , agents  $\Sigma$ , a desired formation  $\zeta^* \in \text{Im}(\mathcal{E}^T)$ , and an error margin  $\varepsilon$ , find a controller  $\Pi$  so that the relative output vector  $\zeta(t)$  of the network  $(\mathcal{G}, \Sigma, \Pi)$  converges to some  $\zeta_0$  such that  $\|\zeta^* - \zeta_0\| \leq \varepsilon$ .*

By choosing suitable error margins  $\varepsilon$ , practical formation control (compared to formation control) comprises no restriction or real drawback in any application case. Therefore, solving the practical formation control problem constitutes an interesting problem especially for unknown dynamics of the agents. Thus, we strive to develop an algorithm solving this practical formation control problem without a model of the agents while still providing rigorous guarantees.

The underlying idea of our approach is amplifying the controller output. Consider the scenario depicted in Fig. 2, where the graph  $\mathcal{G}$ , the agents  $\Sigma$  and the nominal controller  $\Pi$  are fixed, and the gain matrix  $A$  is a diagonal matrix  $A = \text{diag}(\{a_e\}_{e \in \mathcal{E}})$  with positive entries. We will show in the following that when the gains  $a_e$  become large enough, then the controller dynamics  $\Pi$  become much more emphasized than the agent dynamics  $\Sigma$ . By correctly choosing the nominal controller  $\Pi$  according to  $\zeta^*$ , we can hence achieve arbitrarily close formations to  $\zeta^*$ , as the effect of the agents on the closed-loop dynamics will be dampened. We denote the diffusively-coupled system in Fig. 2 as the 4-tuple  $(\mathcal{G}, \Sigma, \Pi, A)$ , or as  $(\mathcal{G}, \Sigma, \Pi, a)$  where  $a$  is the vector of diagonal entries of  $A$ . In case  $A$  has uniform gains, i.e.,  $A = \alpha I$ , we'll denote the system as  $(\mathcal{G}, \Sigma, \Pi, \alpha \mathbf{1}_n)$ . In order to apply the network optimization framework of Theorem 1, we make the following assumption:

**Assumption 1.** *The agents  $\{\Sigma_i\}_{i \in \mathcal{V}}$  are all MEIP, and the nominal controllers  $\{\Pi_e\}_{e \in \mathcal{E}}$  are all output-strictly MEIP.*

Before expanding on the suggested controller design, we want to discuss Assumption 1. In practice, it might not be known whether an agent is MEIP. Therefore, we discuss on how to either verify MEIP for the agents, or determine their shortage of passivity if they are not MEIP. We also discuss how to passivize the agents in the latter case.

First, in some occasions, we actually do have some model for the agents, which might be obscure or uncertain. For example, one might know that an agent can be modeled by some gradient system, or some Euler-Lagrange system, but the exact model is unknown due to uncertainty on the characterizing parameters. In that case, we can use analytical

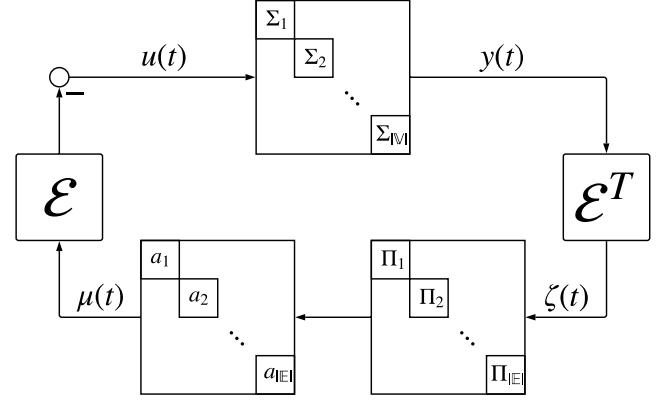


Fig. 2. Block-diagram of the diffusively-coupled network  $(\Sigma, \Pi, \mathcal{G}, A)$ .

results to check if the agents are MEIP. To exemplify this idea, we show how a very rough model can be used to prove that a system is MEIP.

**Proposition 1.** *Consider a control-affine SISO dynamical system of the form*

$$\dot{x} = -f(x) + g(x)u; \quad y = h(x), \quad (3)$$

where we assume that  $g(x) > 0$  for all  $x$ , and that the functions  $f/g, h : \mathbb{R} \rightarrow \mathbb{R}$  are continuous monotone ascending functions. Moreover, assume that either  $\lim_{|x| \rightarrow \infty} |f(x)/g(x)| = \infty$  or  $\lim_{|x| \rightarrow \infty} |h(x)| = \infty$ . Then (3) is MEIP.

The proof of the proposition is available in the appendix. See also [35] for a treatment on gradient systems with oscillatory terms. More generally, one can use an obscure model to give an estimate about equilibrium-independent passivity indices using similar ideas.

Another approach for verifying Assumption 1 is learning input-output passivity properties from trajectories. For LTI systems, the shortage of passivity can be asymptotically revealed by iteratively probing the agents and measuring the output signal as presented in [24] and extended, e.g., in [25]. More recently, it has been shown in [26] that even one input-output trajectory (with persistently exciting input) is sufficient to find the shortage of passivity of an LTI system. For nonlinear agents, one can apply approaches presented in [23], [44], under an assumption on Lipschitz continuity of the steady-state relation. However, for general non-linear systems, this is still a work in progress. It should be noted that for LTI systems, output-strict passivity directly implies output strict MEIP [33].

Using either approaches, we can either find that an agent is MEIP, or that it has some shortage of passivity, and we need to render the agent passive in order to apply the model-free formation control approaches presented in this paper. We can use passifying transformations on the non-passive agent in order to get a passive augmented agent. For example, if the agent has output-shortage of passivity  $s_i > 0$ , we can apply a controller  $C_i : y_i \mapsto \nu_i y_i$  to the agent as in [36], with  $\nu_i > s_i$ , as shown in Fig. 3. It can be shown that the

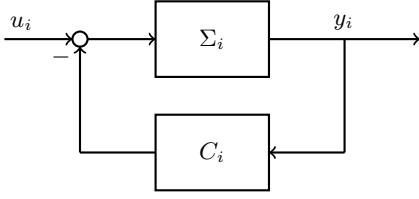


Fig. 3. Passivation of a passivity-short agent using feedback.

augmented agent is output-strictly MEIP in this case. More generally, one could deal with more complex shortages of passivity, namely simultaneous input- and output-shortage of passivity, using more complex transformations [36].

With this discussion and relaxation of Assumption 1, we return to our solution of the practical formation control problem. Recall that we considered closed-loop systems of the form  $(\mathcal{G}, \Sigma, \Pi, a)$ , where  $a$  is a vector of edge gains. From here, the paper diverges into two sections. The next section deals with theory and analysis for uniform edge gains. The following section deals with theory and analysis for the case of heterogeneous edge gains.

#### IV. PRACTICAL FORMATION CONTROL WITH UNIFORM GAINS

We split this chapter into two parts. The first part deals with the theory, and the second part deals with the corresponding implementation of practical formation control synthesis using uniform gains on the edges.

##### A. Theory

We wish to understand the effect of amplification on the steady-state of the closed-loop system. For the remainder of the section, we fix a graph  $\mathcal{G}$ , agents  $\Sigma$  and controllers  $\Pi$  such that Assumption 1 holds. We consider the diffusively coupled system  $(\mathcal{G}, \Sigma, \Pi, \alpha \mathbf{1}_n)$  in Fig. 2, where the gains over all edges are identical and equal to  $\alpha > 0$ , and wish to understand the affect of  $\alpha$ . We let  $K$  and  $\Gamma$  denote the sum of the integral functions of the agents and of the controllers, respectively. We first study the steady-states of this diffusively coupled system.

**Lemma 1.** *Under the assumptions above, the closed-loop system converges to a steady-state, and the steady-state vectors  $y, \zeta$  of the closed-loop system are minimizers of the following optimization problem (OPP):*

$$\begin{aligned} \min_{y, \zeta} \quad & K^*(y) + \alpha \Gamma(\zeta) \\ \text{s.t.} \quad & \mathcal{E}^T y = \zeta. \end{aligned}$$

*Proof.* We define a new stacked controller,  $\bar{\Pi} = \alpha \Pi$ , by cascading the previous controller  $\Pi$  with the gain  $\alpha$ . The resulting controller  $\bar{\Pi}$  is again output-strictly MEIP, and we let  $\bar{\gamma}, \bar{\Gamma}$  denote the corresponding steady-state input-output relation and integral function. Theorem 1 implies that the closed-loop system (with  $\bar{\Pi}$ ) converges to minimizers of (OPP) for the system  $(\mathcal{G}, \Sigma, \bar{\Pi})$ . Hence, we have  $\bar{\gamma}(\zeta) = \alpha \gamma(\zeta)$  for

any  $\zeta \in \mathbb{R}^{|\mathcal{E}|}$ . Integration thus yields  $\bar{\Gamma} = \alpha \Gamma$ , and writing (OPP) for the system  $(\mathcal{G}, \Sigma, \bar{\Pi})$  reads:

$$\begin{aligned} \min_{y, \zeta} \quad & K^*(y) + \alpha \Gamma(\zeta) \\ \text{s.t.} \quad & \mathcal{E}^T y = \zeta. \end{aligned}$$

□

Our goal is to show that when  $\alpha \gg 1$ , the relative output vector  $\zeta$  of the diffusively coupled system  $(\mathcal{G}, \Sigma, \Pi, \alpha \mathbf{1}_n)$  globally asymptotically converges to an  $\varepsilon = \varepsilon(\alpha)$ -ball around the minimizer of  $\Gamma$ , and  $\lim_{\alpha \rightarrow \infty} \varepsilon(\alpha) = 0$ . Thus, if we design the controllers so that  $\Gamma$  is minimized at  $\zeta^*$ , then  $\alpha \gg 1$  provides a solution to the  $\varepsilon$ -practical formation control problem. Indeed, we can prove the following theorem:

**Theorem 2.** *Consider the closed-loop system  $(\mathcal{G}, \Sigma, \Pi, \alpha \mathbf{1}_n)$ , where we assume that the agents are MEIP and the controllers are output-strictly MEIP. Assume  $\Gamma$  has a unique minimizer in  $\text{Im}(\mathcal{E}^T)$ , denoted  $\zeta_1$ . For any  $\varepsilon > 0$ , there exists some  $\alpha_0 > 0$ , such that for all  $\alpha > \alpha_0$  and for all initial conditions, the closed-loop system converges to a vector  $y$  satisfying  $\|\mathcal{E}^T y - \zeta_1\| < \varepsilon$ .*

In order to prove the theorem, we study (OPP) for the diffusively coupled system  $(\mathcal{G}, \Sigma, \Pi, \alpha \mathbf{1}_n)$ , as described in Lemma 1. In order to do so, we need to prove a couple of lemmas. The first deals with lower bounds on the values of convex functions away from their minimizers.

**Lemma 2.** *Let  $U$  be a finite-dimensional vector space and let  $f : U \rightarrow \mathbb{R}$  be a strictly convex function. Denote  $x_0 \in U$  as the unique minimum of  $f$ . Then for any  $\delta > 0$  there exists some  $M > f(x_0)$  such that for any point  $x \in U$ , if  $f(x) < M$  then  $\|x - x_0\| < \delta$ .*

*Proof.* We assume without loss of generality that  $f(x_0) = 0$ . Let  $\mu$  be the minimum of  $f$  on the set  $\{x \in U : \|x - x_0\| = \delta\}$ , which is positive since  $x_0$  is  $f$ 's unique minimum and the set  $\{x \in U : \|x - x_0\| = \delta\}$  is compact. We know that, for any  $y \in U$ , the difference quotient

$$\frac{f(x_0 + \lambda y) - f(x_0)}{\lambda}$$

is an increasing function of  $\lambda > 0$  (see Theorem 23.1 of [42]). Manipulating this inequality implies that for any  $x \in U$ , if  $\|x\| \geq \delta$  then we have that  $f(x) \geq \frac{\|x\|}{\delta} \mu$ , and in particular  $f(x) \geq \mu$  whenever  $\|x\| \geq \delta$ . Thus, if  $f(x) < \mu$  then we must have  $\|x - x_0\| < \delta$ , so we can choose  $M = \mu$  and complete the proof. □

The second lemma deals with minimizers of perturbed versions of convex functions on graphs.

**Lemma 3.** *Fix a graph  $\mathcal{G} = (\mathbb{V}, \mathbb{E})$  and let  $\mathcal{E}$  be its incidence matrix. Let  $K : \mathbb{R}^{|\mathbb{V}|} \rightarrow \mathbb{R}$  be a convex function, and let  $\Gamma : \mathbb{R}^{|\mathcal{E}|} \rightarrow \mathbb{R}$  be a strictly convex function having a unique minimum  $\zeta_1$  when restricted to the set  $\text{Im}(\mathcal{E}^T)$ . For any  $\alpha > 0$ , consider the function  $F_\alpha(y) = K^*(y) + \alpha \Gamma(\mathcal{E}^T y)$ . Then for any  $\varepsilon > 0$ , there exists some  $\alpha_0 > 0$  such that if  $\alpha > \alpha_0$  then all of  $F_\alpha$ 's minima,  $y$ , satisfy  $\|\mathcal{E}^T y - \zeta_1\| < \varepsilon$ .*

*Proof.* By subtracting constants from  $K^*$  and  $\Gamma$ , we may assume without loss of generality that  $\min(K^*) = \min(\Gamma) = 0$ . Choose some  $y_0 \in \mathbb{R}^{|V|}$  such that  $\mathcal{E}^T y_0 = \zeta_1$  and let  $m = K^*(y_0)$ . Note that  $F_\alpha(y_0) = m$ , meaning that if  $y$  is any minimum of  $F_\alpha$ , it must satisfy  $F_\alpha(y) \leq m$ , and in particular  $\Gamma(\mathcal{E}^T y) \leq \frac{m}{\alpha}$ . Now, from Lemma 2 we know that there's some  $M > 0$  such that if  $\Gamma(\mathcal{E}^T y) < M$  then  $\|\mathcal{E}^T y - \zeta_1\| < \varepsilon$ . If we choose  $\alpha_0 = \frac{m}{M}$ , then whenever  $\alpha > \alpha_0$  we have  $\Gamma(\mathcal{E}^T y) < M$ , implying  $\|\mathcal{E}^T y - \zeta_1\| < \varepsilon$ . This completes the proof of the lemma.  $\square$

We now connect the pieces and prove Theorem 2.

*Proof.* Lemma 1 implies that the closed-loop system always converges to a minimizer of (OPP)

$$\begin{aligned} \min_{y, \zeta} \quad & K^*(y) + \alpha \Gamma(\zeta) \\ \text{s.t.} \quad & \mathcal{E}^T y = \zeta. \end{aligned}$$

Lemma 3 proves that there is some  $\alpha_0 > 0$  such that if  $\alpha > \alpha_0$  then all minimizers of (OPP) satisfy  $\|\mathcal{E}^T y - \zeta_1\| < \varepsilon$ . This proves that theorem.  $\square$

**Remark 2.** The parameters  $\varepsilon$  and  $\zeta^*$  can be used to estimate the minimal gain  $\alpha_0$  solving the  $\varepsilon$ -practical formation control problem by following the proofs of Lemma 2 and Lemma 3. Namely,  $\alpha_0 \leq \frac{m}{M}$  where  $M$  is the minimum of  $\Gamma$  on the set  $\{\zeta \in \text{Im}(\mathcal{E}^T) : \|\zeta - \zeta^*\| = \varepsilon\}$ , and  $m = K^*(y_0) - \min_y K^*(y) = K^*(y^*) + K(0)$  where  $y^* \in \mathbb{R}^{|V|}$  is any vector satisfying  $\mathcal{E}^T y^* = \zeta^*$ .

**Corollary 1.** Let  $(\mathcal{G}, \Sigma, \Pi, \alpha \mathbb{1}_n)$  satisfy Assumption 1 and let  $(\mathcal{G}, \Sigma_{\text{Int}}, \Pi)$  be a network comprised of integrator dynamics for each agent. Denote the relative outputs of each system as  $\zeta(t)$  and  $\zeta_{\text{Int}}(t)$  respectively. Then for any  $\varepsilon > 0$ , there exists an  $\alpha_0 > 0$  such that if  $\alpha \geq \alpha_0$ , then the relative outputs  $\zeta(t)$  and  $\zeta_{\text{Int}}(t)$  both converge to constant vectors  $\zeta^*$  and  $\zeta_{\text{Int}}^*$  respectively, and satisfy  $\|\zeta^* - \zeta_{\text{Int}}^*\| \leq \varepsilon$ .

*Proof.* The agents  $\Sigma_{\text{Int}}$  are MEIP. Thus, by Theorem 1, we know that the diffusively-coupled system  $(\mathcal{G}, \Sigma_{\text{Int}}, \Pi)$  converges to a steady-state, and its steady-state output is a minimizer of the associated (OPP) problem. Note that the input-output relation of  $\Sigma_{\text{Int}}$ 's is given via  $k^{-1}(y) = 0$ , meaning the integral function  $K^*$  is the zero function. Thus the associated problem (OPP) is the unconstrained minimization of  $\Gamma(\mathcal{E}^T y)$ , meaning that the system  $(\mathcal{G}, \Sigma_{\text{Int}}, \Pi)$  converges, and its output converges to a minimizer of  $\Gamma(\mathcal{E}^T y)$ , i.e., its relative output  $\zeta(t)$  converges to the minimizer of  $\Gamma$  on  $\text{Im}(\mathcal{E}^T)$ . Applying Theorem 2 now completes the proof.  $\square$

**Remark 3** (Almost Data-free control). Corollary 1 can be thought of as a synthesis procedure. Indeed, we can solve the synthesis problem as if the agents were simple integrators, and then amplify the controller output by a factor  $\alpha$ . The corollary shows that for any  $\varepsilon > 0$ , there is a threshold  $\alpha_0 > 0$  such that if  $\alpha > \alpha_0$ , then the closed-loop system converges to an  $\varepsilon$ -neighborhood of  $\zeta^*$ . It is important to note that we only know that  $\alpha_0$  exists as long as the agents are MEIP. Computing an estimate on  $\alpha_0$ , however, requires one to conduct a few experiments.

There are a few possible approaches to try and eliminate this requirement. One can try an iterative scheme, in which the edge gains are updated between iterations. Gradient-descent and extremum-seeking approaches are discussed in the next section (see Algorithm 3), but both require to measure the system between iterations.

Another approach is to update the edge gains on a much slower time-scale than the dynamics of the system. This results in a two time-scale dynamical system, where the gains  $a_e$  of the system  $(\mathcal{G}, \Sigma, \Pi, a)$  are updated slowly enough to allow the system to converge. Taking  $a_e$  as uniform gains of size  $\alpha$ , and slowly increasing  $\alpha$ , assures that eventually,  $\alpha > \alpha_0$ , so the system will converge  $\varepsilon$ -close to  $\zeta^*$ . The only data we do need is whether or not the system has already converged to an  $\varepsilon$ -neighborhood of  $\zeta^*$ , to know whether  $\alpha$  should be updated or not. This requires no data on the trajectories themselves, nor information on the specific steady-state limit. This results in an essentially data-free solution of the practical formation control problem, in which the only data needed is whether or not the control goal has been achieved. Moreover, the algorithm is valid as long as the agents are known to be MEIP.

## B. Data-Driven Determination of Gains

In the previous subsection, we introduced a formula for a uniform gain  $\alpha$  described by the ratio of  $m$  and  $M$ , that solves the practical formation problem, where  $m$  and  $M$  are as defined in Remark 2. The parameter  $M$  depends on the integral function  $\Gamma$  of the controllers, evaluated on well-defined points, namely  $\{\zeta \in \text{Im}(\mathcal{E}^T) : \|\zeta - \zeta^*\| = \varepsilon\}$ . Thus we can compute  $M$  exactly with no prior knowledge on the agents. This is not the case for the parameter  $m$ , which depends on the integral function of the agents. Without knowledge of any model of the agents, we need to obtain an estimate of  $m$  solely on the basis of input-output data from the agents.

From Remark 2 above, we know that  $m = \sum_{i=1}^n (K_i^*(y_i^*) + K_i(0)) = \sum_{i=1}^n m_i$  for some  $y^* \in \mathbb{R}^n$  such that  $\mathcal{E}^T y^* = \zeta^*$ . Without any model of the agents,  $m$  cannot be computed directly, but we can receive an upper bound on  $m$  from measured input-output trajectories via the inverse relations  $k_i^{-1}$ ,  $i = 1, \dots, n$ .

**Proposition 2.** Let  $(u_i^*, y_i^*)$ ,  $(u_{i,1}, y_{i,1})$ ,  $(u_{i,2}, y_{i,2})$ ,  $\dots$ ,  $(u_{i,r}, y_{i,r})$  and  $(0, y_{i,0})$  be steady-state input-output pairs for agent  $i$ , for some  $r \geq 0$ . Then:

$$m_i \leq u_{i,1}(y_{i,1} - y_{i,0}) + \dots + u_{i,r}(y_{i,r} - y_{i,r-1}) + u_i^*(y^* - y_{i,r}).$$

*Proof.* We prove the claim by induction on the number of steady-state pairs,  $r + 2$ . First, consider the case  $r = 0$  of two steady-state pairs. First, because  $(0, y_{i,0})$  is a steady-state pair, we know that  $K_i(0) = -K_i^*(y_{i,0})$  by Fenchel duality. Similarly,  $K_i(u_i^*) = u_i^* y_i^* - K_i^*(y_i^*)$ . Thus,

$$m_i = K_i^*(y_i^*) + K_i(0) = K_i^*(y_i^*) - K_i^*(y_{i,0}) \leq u_i^*(y^* - y_{i,0}),$$

where we use the inequality  $K_i^*(b) - K_i^*(c) \geq k_i^{-1}(c)(b - c)$  for  $b = y_{i,0}$  and  $c = y_i^*$ . Now, we move to the case  $r \geq 1$ . We write  $m_i$  as  $(K_i^*(y_i^*) - K_i^*(y_{i,r})) + (K_i^*(y_{i,r}) - K_i(0))$ . The first element can be shown to be smaller or equal than  $u_i^*(y^* - y_{i,r})$  using the inequality  $K_i^*(b) - K_i^*(c) \geq k_i^{-1}(c)(b - c)$  for

$b = y_{i,r}$  and  $c = y_i^*$ . The second element is smaller or equal than  $u_{i,1}(y_{i,1} - y_{i,0}) + \dots + u_{i,r}(y_{i,r} - y_{i,r-1})$  by induction hypothesis, as we use a total of  $r + 1$  steady-state input-output pairs. Thus,  $m_i$  is smaller or equal than the sum of the two bounds, which is equal to  $u_{i,1}(y_{i,1} - y_{i,0}) + \dots + u_{i,r}(y_{i,r} - y_{i,r-1}) + u_i^*(y^* - y_{i,r})$ .  $\square$

**Remark 4.** If we only have two steady-state pairs,  $(u_i^*, y_i^*)$  and  $(0, y_{i,0})$ , the estimate on  $m_i$  becomes  $m_i \leq u_i^*(y_i^* - y_{i,0})$ . Thus two steady-state pairs, corresponding to two measurements/experiments, are enough to yield a meaningful bound on  $m_i$ . However, it is important to note that more experiments yield better estimates of  $m_i$ , i.e., if  $r \geq 1$  then the estimate in the theorem is better than the one above as long as  $(y_{i,0}, y_{i,1}, \dots, y_{i,r}, y_i^*)$  is a monotone series.

With Remark 4, we can hence compute an upper bound on  $m$  from the two steady-state pairs  $(u_i^*, y_i^*)$  and  $(0, y_{i,0})$  of each agent. In the following, we present two methods on how to actually obtain the required steady-state input-output pairs  $(0, y_{i,0})$  and  $(u_i^*, y_i^*)$  of the agents.

We would like to estimate  $m_i$  from above by computing  $y_{i,0}$  and  $u_i^*$ . Designing experiments to measure these quantities are possible, but can require additional information on the plant, e.g. output-strict passivity. Instead, we opt for a different approach and try to estimate  $y_{i,0}$  and  $u_i^*$  instead of computing them directly. This is described in Algorithm 1.

Algorithm 1 applies Remark 4 in order to bound  $m_i$  from above. It does so by using the monotonicity of the steady-state input-output relation to bound  $u_i^*$  and  $y_{i,0}$  from above and below, as computing the exact values of  $u_i^*$  and  $y_{i,0}$  might not be feasible only from experiments. It is important to note that the closed-loop experiments are done with output-strictly MEIP controller, which assure that the closed-loop system indeed converges. We prove the following:

**Proposition 3.** The output  $\mathfrak{m}_i$  from Algorithm 1 is an upper bound on  $m_i$ .

*Proof.* First, we show that the closed-loop experiments conducted by the algorithm indeed converge. The plant  $\Sigma_i$  is assumed to be passive with respect to any steady-state input-output pair it possesses. Moreover, the static controller  $u = \beta_i(y - y_{\text{ref}})$  is output-strictly passive with respect to any steady-state input-output pair it possesses. Thus it's enough to show that the closed-loop system has a steady-state, which will prove convergence as this is a feedback connection of a passive system with an output-strictly passive system. Indeed, a steady-state input-output pair  $(u_i, y_i)$  of the system needs to satisfy  $u_i \in k_i^{-1}(y_i)$  and  $u_i = -\beta_i(y_i - y_{\text{ref}})$ . Thus it's enough to show that  $-\beta_i(y_i - y_{\text{ref}}) \in k_i^{-1}(y_i)$  has a solution. This is equivalent to

$$0 \in k_i^{-1}(y_i) + \beta_i(y_i - y_{\text{ref}}) = \nabla \left( K_i^*(y_i) + \frac{\beta_i}{2}(y_i - y_{\text{ref}})^2 \right),$$

so  $y_i$  exists and is equal to the minimizer of  $K_i^*(y_i) + \frac{\beta_i}{2}(y_i - y_{\text{ref}})^2$ . This shows that the closed-loop experiments converge. Thus the algorithm halts, and it remains to show that it outputs an upper-bound on  $m_i$ .

---

**Algorithm 1:** Estimating  $m_i$  for an MEIP Agent

---

```

1 Run the closed-loop system in Fig. 4 with  $\beta_i$  small and
    $y_{\text{ref}} = \frac{1}{\beta_i}$ ;
2 Wait for convergence, and measure the steady-state output  $y_{i,+}$ 
   and the steady-state input  $u_{i,+}$ ;
3 Run the closed-loop system in Fig. 4 with  $\beta_i$  small and
    $y_{\text{ref}} = -\frac{1}{\beta_i}$ ;
4 Wait for convergence, and measure the steady-state output  $y_{i,-}$ 
   and the steady-state input  $u_{i,-}$ ;
5 if  $y_{i,+} < y_i^*$  then
6   Run the closed-loop system in Fig. 4 with  $\beta_i = 1$  and
    $y_{\text{ref}} \gg y_i^*$ ;
7   Wait for convergence, and measure the steady-state input
    $u_{i,2}$  and output  $y_{i,2}$ ;
8 else
9   if  $y_{i,-} > y_i^*$  then
10    Run the closed-loop system in Fig. 4 with  $\beta_i = 1$  and
     $y_{\text{ref}} \ll y_i^*$ ;
11    Wait for convergence, and measure the steady-state
    input  $u_{i,2}$  and output  $y_{i,2}$ ;
12  else
13    Define  $u_{i,2} = u_{i,+}$  and  $y_{i,2} = y_{i,+}$ ;
14  end
15 end
16 Sort the array  $\{u_{i,-}, u_{i,+}, u_{i,2}\}$ . Denote the result by
    $U = \{U_1, U_2, U_3\}$ ;
17 Sort the array  $\{y_{i,-}, y_{i,+}, y_{i,2}\}$ . Denote the result by
    $Y = \{Y_1, Y_2, Y_3\}$ ;
18 if  $U_2 > 0$  then
19   Define  $\underline{y}_{i,0} = Y_1$  and  $\overline{y}_{i,0} = Y_2$ ;
20 else
21   if  $U_2 < 0$  then
22     Define  $\underline{y}_{i,0} = Y_2$  and  $\overline{y}_{i,0} = Y_3$ ;
23   else
24     Define  $\underline{y}_{i,0} = Y_2$  and  $\overline{y}_{i,0} = Y_2$ ;
25   end
26 end
27 if  $Y_2 > y_i^*$  then
28   Define  $\underline{u}_i^* = U_1$  and  $\overline{u}_i^* = U_2$ ;
29 else
30   if  $Y_2 < y_i^*$  then
31     Define  $\underline{u}_i^* = U_2$  and  $\overline{u}_i^* = U_3$ ;
32   else
33     Define  $\underline{u}_i^* = U_2$  and  $\overline{u}_i^* = U_2$ ;
34   end
35 end
36 return  $\mathfrak{m}_i$  as the maximum over  $\omega(y_i^* - v)$ , where
    $\omega \in \{\underline{u}_i^*, \overline{u}_i^*\}$  and  $v \in \{\underline{y}_{i,0}, \overline{y}_{i,0}\}$ ;

```

---

Using Remark 4, it's enough to show that  $y_{i,0} \in [\underline{y}_{i,0}, \overline{y}_{i,0}]$  and  $u_i^* \in [\underline{u}_i^*, \overline{u}_i^*]$ . To do so, we first claim that  $U_1 \leq u_i^* \leq U_3$  and  $Y_1 \leq y_{i,0} \leq Y_3$ . We first show that  $Y_1 \leq y_{i,0}$ , by showing that  $y_{i,-} \leq y_{i,0}$ . Indeed, because  $k_i$  is a monotone map, this is equivalent to saying that  $u_{i,-} \leq 0$ . By the structure of the second experiment, the steady-state input is close to  $-1$ , and in particular smaller than 0. The inequality  $y_{i,0} \leq y_{i,+}$  is proved similarly. We note that because  $u_{i,-} \approx -1$  and  $u_{i,+} \approx 1$ , we have  $u_{i,-} \leq u_{i,+}$  and thus  $y_{i,-} \leq y_{i,+}$  as  $k_i$  is monotone.

Next, we prove that  $U_1 \leq u_i^*$ . By monotonicity of  $k_i$ , this is equivalent to  $Y_1 \leq y_i^*$ . Because  $y_{i,-} \leq y_{i,+}$ , it's enough to show that either  $y_{i,-} \leq y_i^*$  or  $y_{i,2} \leq y_i^*$ . If the first case is true, then the proof is complete. Otherwise,  $y_{i,-} > y_i^*$ , so

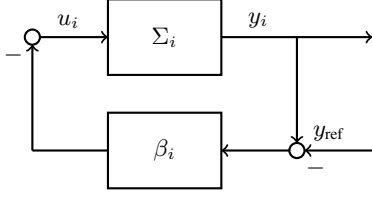


Fig. 4. Experimental setup of the closed-loop experiment for estimating  $m_i$  as used in Algorithm 1.

the algorithm finds  $y_{i,2}$  by running the closed-loop system in Fig. 4 with  $\beta_i = 1$  and  $y_{\text{ref}} \ll y_i^*$ . The increased coupling strength implies that the steady-state output  $y_{i,2}$  should be close to  $y_{\text{ref}}$ , which is much smaller than  $y_i^*$ . Thus  $y_{i,2} < y_i^*$ , which shows that  $Y_1 \leq y_1^*$ , or equivalently  $U_1 \leq u_1^*$ . The proof that  $u_1^* \leq U_3$  is similar. This completes the proof of the proposition.  $\square$

**Remark 5.** The second part of Algorithm 1, namely from Step 16 until the end, can be used to improve the estimates on  $u_i^*$  and  $y_{i,0}$ . Namely, we run another experiment, in which the agent converges to a steady-state input-output pair  $(\hat{u}_i, \hat{y}_i)$ . One then defines the array  $U = \{\underline{u}_i^*, \bar{u}_i^*, \hat{u}_i\}$  and  $Y = \{\underline{y}_{i,0}, \bar{y}_{i,0}, \hat{y}_i\}$ , and applies this last part (line 16-36) once more. If  $\hat{u}_i$  is not between  $\underline{u}_i^*$  and  $\bar{u}_i^*$ , (or equivalently,  $\hat{y}_i$  is not between  $\underline{y}_{i,0}$  and  $\bar{y}_{i,0}$ ), then we do not improve our estimate of  $m_i$ . Otherwise, we shrink the estimated intervals containing  $u_i^*$  and  $y_{i,0}$ , and thus improve our estimate of  $m$ . Doing this iteratively allows to exactly compute  $u_i^*$  and  $y_i^*$ , which would be not advisable in practice due to the huge amount of necessary experiments.

We saw that  $m_i$  can be bounded using no more than three experiments for general MEIP agents. However, we can improve on that if we somehow know that the agent is LTI. To be precise, we have the following proposition.

**Proposition 4.** Suppose that the agent  $\Sigma_i$  is known to be both MEIP and LTI. Let  $(\tilde{u}, \tilde{y})$  be any steady-state input-output pair for which either  $u_1 \neq 0$  or  $y_1 = 0$ .<sup>1</sup> Then  $m_i = \frac{(y_i^*)^2 \tilde{u}}{2\tilde{y}}$ . Thus  $m_i$  can be exactly calculated using a single experiment.

*Proof.* Indeed, [32], [35] show that in this case,  $k$  is a linear function, and the system state matrix is Hurwitz. Moreover, unless the transfer function of the agent is 0,  $k^{-1}$  is a linear function  $k^{-1}(y) = sy$  for some  $s > 0$  [37]. Thus  $K^*(y) = \frac{s}{2}y^2$ . Now,  $k^{-1}(0) = s \cdot 0 = 0$ , so  $(0, 0)$  is a steady-state input-output pair, meaning that  $y_{i,0} = 0$ . Moreover, we know that  $\tilde{u} = s\tilde{y}$ , and not both are zero, so we conclude that  $\tilde{y} \neq 0$ , and that  $s = \frac{\tilde{u}}{\tilde{y}}$ . Thus,  $K_i^*(y_{i,0}) = K_i^*(0) = 0$  and  $K_i^*(y_i^*) = \frac{s}{2}(y_i^*)^2 = \frac{s}{2}y^2$ . This completes the proof, as  $m_i = K_i^*(y_i^*) - K_i^*(y_{i,0})$ .  $\square$

We conclude this chapter with Algorithm 2 for solving the practical formation control problem using the single-gain amplification scheme, which is applied to two case studies in Section VI.

---

#### Algorithm 2: Synthesis Procedure for Practical Formation Control

---

- 1 Choose some output-strictly MEIP controllers  $\Pi_e$  such that the integral function  $\Gamma$  has a single minimizer  $\zeta^*$  when restricted to the set  $\text{Im}(\mathcal{E}^T)$ ;
  - 2 Choose some  $y^* \in \mathbb{R}^n$  such that  $\mathcal{E}^T y^* = \zeta^*$ ;
  - 3 **for**  $i = 1, \dots, n$  **do**
  - 4 | Run Algorithm 1. Let  $m_i$  be the output;
  - 5 **end**
  - 6 Let  $m = \sum_{i=1}^n m_i$ ;
  - 7 Compute  $M = \min\{\zeta \in \text{Im}(\mathcal{E}^T) : \|\zeta - \zeta^*\| = \varepsilon\}$ ;
  - 8 Compute  $\alpha = m/M$ ;
  - 9 **return** the controllers  $\{\alpha \Pi_e\}_{e \in \mathbb{E}}$ ;
- 

**Remark 6.** Step 1 of the algorithm allows almost complete freedom of choice for the controllers. One possible choice are the static controllers  $\mu_e = \zeta_e - \zeta_e^*$ . Moreover, if  $\Pi_e$  is any MEIP controller for each  $e \in \mathbb{E}$ , and  $\gamma_e(\zeta_e) = 0$  has a unique solution for each  $e \in \mathbb{E}$ , then the “formation reconfiguration” scheme from [34] suggests a way to find the required controllers using mild augmentation.

**Remark 7.** The algorithm allows one to choose any vector  $y^*$  such that  $\mathcal{E}^T y^* = \zeta^*$ . All possible choices lead to some gain  $\alpha$  which assures a solution of the practical formation control problem, but some choices yield better results (i.e., smaller gains) than others. The optimal  $y^*$ , minimizing the estimate  $a$ , can be found as the minimizer of the problem  $\min\{K^*(y) : \mathcal{E}^T y = \zeta^*\}$ , which we cannot compute using data alone. One can use physical intuition to choose a vector  $y^*$  which is relatively close to the actual minimizer, but the algorithm is still valid no matter which  $y^*$  is chosen.

## V. ITERATIVE PRACTICAL FORMATION CONTROL APPLYING DIFFERENT GAINS ON DIFFERENT EDGES

Let us revisit Fig. 2 and let  $A = \text{diag}(\{a_e\}_{e \in \mathbb{E}})$  with positive, but distinct entries  $a_e$ . These additional degrees of freedom can be used, for example, to reduce the conservatism and retrieve a smaller norm of the adjustable gain vector  $a$  while still solving the practical formation control problem. It follows directly from Theorem 2 that there always exists a bounded vector  $a$  that solves the practical formation control problem. However, the question remains how the entries of  $a$  can be chosen based only on knowledge of input-output data and passivity properties.

Our idea here is to probe our diffusively coupled system for given gains  $a_e$  and adjust the gains according to the resulting steady-state output. By iteratively performing experiments in this way, we strive to find controller gains that solve the practical formation problem. This idea and approach is tightly connected to iterative learning control, where one iteratively applies and adjusts a controller to improve the performance of the closed-loop for a repetitive task [45]. Our approach here is based on passivity and network optimization with only requiring the possibility to perform iterative experiments.

One natural idea in this direction is to define a cost function that penalizes the distance of the resulting steady-state to the desired formation control goal and then apply

<sup>1</sup>e.g., by running the system in Fig. 4 with some  $\beta > 0$  and  $y_{\text{ref}} \neq 0$



a gradient descent approach, adjusting the gain  $a$  for each experiment. However, to obtain the gradient of  $\|\mathcal{E}^T y(a) - \zeta^*\|^2$  with respect to the vector  $a$ , where  $y(a)$  is the steady-state output of  $(\mathcal{G}, \Sigma, \Pi, a)$ , one requires knowledge of the inverse relations  $k_i^{-1}$  for all  $i = 1, \dots, n$ . With no model of the agents available, a direct gradient descent approach is hence infeasible. Therefore, we present in the following a simple iterative multi-gain control scheme without knowledge on the exact steepest descent direction.

We start off with an arbitrarily chosen gain vector  $a_0$  with only positive entries. Due to Assumption 1, the closed-loop converges to a steady state. According to the measured state, the idea is then to iteratively perform experiments and update the gain vector until we reach our control goal, i.e., practical formation control. The update formula can be summarized by

$$a_e^{(j+1)} = a_e^{(j)} + h v_e, \quad e \in \mathbb{E}, \quad (4)$$

where  $h > 0$  is the step size and  $v$ , with entries  $v_e$ ,  $e = 1, \dots, |\mathbb{E}|$ , is the update direction. We denote the  $e$ -th entry of  $\mathcal{E}^T y$  as  $f_e$  and choose  $v$  in each iteration such that

$$v_e = \begin{cases} \frac{f_e - \zeta_e^*}{\gamma_e(f_e)} & \gamma(f_e) \neq 0 \\ 0 & \text{otherwise} \end{cases}, \quad (5)$$

for all  $e = 1, \dots, |\mathbb{E}|$ . If  $k^{-1}$  and  $\gamma$  are differentiable functions, then we claim that  $F(a) = \|\mathcal{E}^T y(a) - \zeta^*\|^2$  decreases in the direction of  $v$ , i.e.,  $v^T \nabla F(a) < 0$ . This leads to a multi-gain distributed control scheme, using (4) with (5), which is summarized in Algorithm 3. This multi-gain distributed control scheme is guaranteed to solve the practical formation problem after a finite number of iterations, which is summarized in the following theorem.

---

**Algorithm 3:** Practical Formation control with derivative-free optimization

---

```

1 Initialize  $a^{(0)}$ , e.g. with  $\mathbb{1}_{|\mathbb{E}|}$ ;
2 Choose step size  $h$  and set  $j = 0$ ;
3 while  $F(a) = \|\mathcal{E}^T y(a) - \zeta^*\|^2 > \varepsilon$  do
4   Apply  $a^{(j)}$  to the closed loop;
5   Compute  $v_e = \begin{cases} \frac{f_e - \zeta_e^*}{\gamma_e(f_e)} & \gamma(f_e) \neq 0 \\ 0 & \gamma(f_e) = 0 \end{cases} \quad \forall e$ ;
6   Update  $a_e^{(j+1)} = a_e^{(j)} + h v_e$ ,  $j = j + 1$ ;
7 end
8 return  $a$ 
```

---

**Theorem 3.** Suppose that the functions  $k^{-1}$ ,  $\gamma$  are differentiable, and that there exists an agent  $i_0 \in \mathbb{V}$  such that  $\frac{dk_{i_0}^{-1}}{dy_{i_0}} > 0$  for any point  $y_{i_0} \in \mathbb{R}$ . Moreover, assume that  $\frac{d\gamma_e}{d\zeta_e} > 0$  for any  $e \in \mathbb{E}$ ,  $\zeta_e \in \mathbb{R}$ . Then

$$v^T \nabla F(a) \leq 0,$$

with  $v, F$  as defined in Algorithm 3 (and equality if and only if  $\mathcal{E}^T y(a) = \zeta^*$ ). Furthermore, if the step size  $h > 0$  is small enough, then the Algorithm 3 halts after finite time, providing a gain vector that solves the practical formation control problem.

*Sketch of proof.* The proof is based on showing that  $\nabla F$  can be written as  $-\text{diag}(\gamma(f))X(y(a))(f - \zeta^*)$ , where  $X(y(a))$  is a positive-definite matrix depending on  $y(a)$ . We can now show that  $v^T \nabla F \leq 0 = -(f - \zeta^*)^T X(y(a))(f - \zeta^*) \leq 0$ . The full proof of Theorem 3 is available in the appendix.  $\square$

Algorithm 3 together with the theoretical results from Theorem 3 provide us with a very simple and distributed, iterative control scheme with theoretical guarantees. Note also, that the steady-states of the agents are independent of their initial condition. For each iteration, the agents can hence also start from the position they converged to at the last iteration. This can be interpreted similarly to Remark 3, where gains are updated on a slower time scale than convergence of the agents. However, instead of only the information whether practical formation control is achieved, we generally need the actual difference  $\mathcal{E}^T y - \zeta^*$  that is achieved with the current controller in each iteration. In the special case of a proportional controllers  $\mu_e = \zeta_e - (\zeta^*)_e$ , yielding  $v_e = 1$ , we retrieve the exact controller scheme proposed in Remark 3.

An alternative gradient-free control scheme is the extremum seeking framework as presented in [46]. Assuming that  $k^{-1}$  and  $\gamma$  are twice continuously differentiable, a step in the direction of steepest descent is approximated every  $4|\mathbb{E}|$  steps (cf. [46, Theorem 1]). While the extremum seeking framework approximates the steepest descent (and the simple multi-gain approach only guarantees a descending direction), it also requires large amounts of experiments per approximated gradient step. Furthermore, the algorithm as presented in [46] cannot be computed in a purely distributed fashion. Therefore, the simple distributed control scheme in Algorithm 3 displays significant advantages in the present problem setup.

## VI. SIMULATIONS

We will present two extensive case studies. On each case, we apply the presented single-gain and multi-gain approach. The first example considers a class of underactuated vehicles trying to coordinate their velocity in presence of drag and external forces. The second example studies the model-free cooperative control of a neural network.

### A. Velocity Coordination in Vehicles with Drag and Exogenous Forces

Consider a collection of 5 one-dimensional robots, each modeled by a double integrator  $G(s) = \frac{1}{s^2}$ . The robots try to coordinate their velocity. Each of them has its own drag profile  $f(\dot{p})$ , which is unknown to the algorithm, but it is known that  $f$  is increasing and  $f(0) = 0$ . Moreover, each vehicle experiences external forces (e.g., wind, and being placed on a slope). The velocity of the vehicles is governed by the equation

$$\Sigma_i : \begin{cases} \dot{x}_i &= -f_i(x_i) + u_i + w_i \\ y_i &= x_i, \end{cases} \quad (6)$$

where  $x_i$  is the velocity of the  $i$ -th vehicle,  $f_i$  is its drag model,  $w_i$  are the exogenous forces acting on it,  $u_i$  is the control input, and  $y_i$  is the measurement. In the simulation, the drag models  $f_i$  are given by  $c_d|x|$ , where the drag coefficient

$c_d$  is chosen as a log-uniform value between 0.1 and 1. We assume that the vehicles are light, so the wind accelerates the vehicles by a non-negligible amount. Thus, the exogenous input  $w_i$  is randomly chosen between  $-2$  and  $2$ . We wish to achieve velocity consensus, with error no greater than  $\epsilon = 1$ . We consider a diffusive coupling of the system. We use the cycle graph  $\mathcal{G} = \mathcal{C}_5$ , and we choose proportional controllers  $\zeta_e = \mu_e$  with gain equal to 1.

We apply the amplification scheme presented in Algorithm 2 and choose the consensus value  $y_i^* = 1.5 \text{ m/sec}$  to use in the estimation algorithm. Note that the plants are MEIP, but not output-strictly MEIP. We use Algorithm 1 to estimate the needed uniform gain  $\alpha$ . In all cases, the first and second experiments are conducted with  $\beta_i = 0.01$ , and  $y_{\text{ref}} = \pm 100$ . Based on the results of the previous experiments, we run a third experiment on each of the agents for which this is required, this time with  $\beta_i = 1$  and  $y_{\text{ref}} = \pm 10$ , where the sign is chosen according to Algorithm 1. The experimental results of the five plants are available in Figure 5.

We now estimate each  $m_i$  for  $i = 1, \dots, 5$  using Remark 4. For example, for agent 2 we get the three steady-state input-output pairs  $(1.0167, -1.6748)$ ,  $(-0.9586, -4.1426)$ , and  $(4.9341, 5.0659)$ . Monotonicity implies that it has steady-states  $(u_1^*, y_1^*) = (u_1^*, 1.5)$  and  $(0, y_{1,0})$  with  $1.0168 \leq u_1^* \leq 4.9341$  and  $-4.1426 \leq y_{1,0} \leq -1.6748$ . Thus we can estimate  $m_2 \leq 4.9341 \cdot (1.5 - (-4.1426)) = 27.8412$ . Similarly, we estimate  $m_1, m_3, m_4, m_5$ , and get  $m_1 = 17.4568, m_3 = 2.1153, m_4 = 2.0410, m_5 = 13.0345$ . Thus, their sum is  $m = 62.4888$ .

As for estimating  $M$ , we have  $\Gamma_e(\zeta_e) = \zeta_e^2$ , so  $\Gamma(\zeta) = \|\mathbb{E}\|\zeta\|^2$ . The minimum is at  $x_0 = 0$ , and by definition we have  $M = \min_{x \in \text{Im}(\mathcal{E}^T): \|x - x_0\| = \epsilon} \Gamma(x) = \epsilon^2$ . Thus, we get  $\alpha = \frac{m}{M} = \frac{m}{5\epsilon^2} = 12.47$ . To verify the algorithm, we run the closed-loop system  $(\mathcal{G}, \Sigma, \Pi, \alpha \mathbb{1})$  with the gain  $\alpha$  we found. The results are available in Figure 6. One can see that the overall control goal is achieved - the agents converge to a steady-state which is  $\epsilon$ -close to consensus. However, it should be noted that the agents actually converge to a much closer steady-state than predicted by the algorithm. Namely, the distance of the steady-state output from consensus is roughly 0.1, much smaller than 1. Thus, the algorithm probably overestimates the minimal gain  $\alpha$  needed by at least one order of magnitude. One can mitigate this by using more experiments to better estimate  $m_i$ , as mentioned in Proposition 2 or in Remark 5. For comparison, running the algorithm with  $y^* = 0$  gives  $\alpha = 16.07$  and  $y_i^* = 1.25 \text{ m/sec}$  gives  $\alpha = 12.40$ .

As seen above, the main factor for  $\alpha$ 's size is the second agent, which contributes about 45% to the size of  $m$ . Thus we wish to reduce  $m_2$  size by using additional experiment. Running a fourth experiment (just on agent #2 with  $\beta_i = 1$  and  $y_{\text{ref}} = 4.5$  gave the steady-state input-output pair  $(2.1577, 2.3423)$ . Estimating  $m_i$  using Remark 5 now gives  $m_i = 11.96$ , which in turn gives  $\alpha = 9.33$ . Thus one additional experiment on a single agent allowed us to reduce the value of  $\alpha$  by about 25%.

Altogether we could show that Algorithm 2 manages to solve the practical consensus problem of vehicles, affected by drag and exogenous inputs, without using any model for the

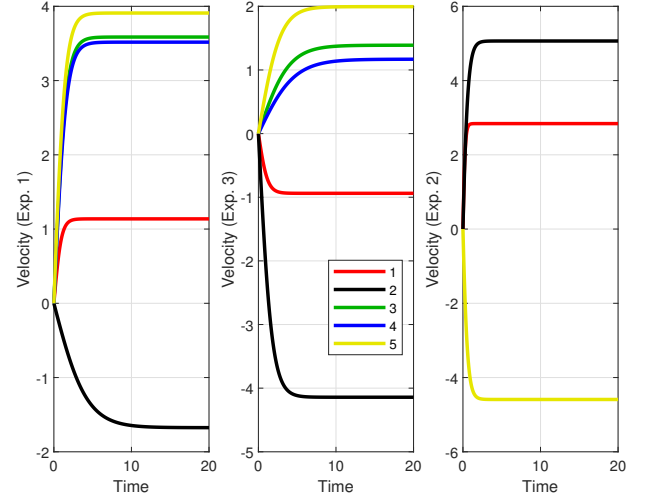


Fig. 5. Results of First Set of Experiments for the Vehicles

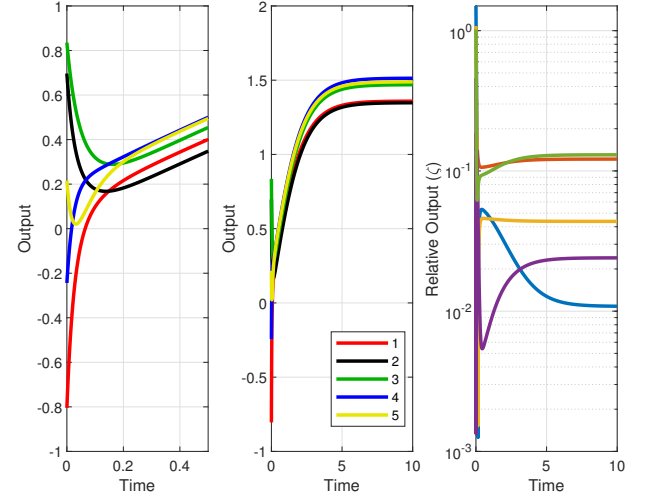


Fig. 6. The Closed-Loop with Uniform Gain  $\alpha = 12.47$ . The two leftmost graphs plot the agents' trajectories over 0.5 seconds and over 10 seconds. The rightmost graphs plots the relative outputs.

agents, while conducting very few experiments for each agent. However, it overestimates the required coupling needed to achieve practical consensus, and thus has unnecessarily large energy consumption. The trajectories of the closed loop system with the new gain are available in Figure 7.

Let us now apply the iterative multi-gain control strategy. We start with  $a^{(0)} = 0.1 \otimes \mathbb{1}_{|\mathbb{E}|}$ , we choose the step size  $h = 0.1$  and apply Algorithm 3. In fact, since  $\zeta^* = 0$  and  $\zeta_e = \mu_e$ , we receive  $v = \mathbb{1}_{|\mathbb{E}|}$ , which constitutes the special case where our iterative scheme yields the controller scheme proposed in Remark 3. The corresponding norm of the gain vector and the resulting  $\epsilon$  in each iteration is illustrated in Fig. 8. After 10 iterations, we already arrive at a vector, which solves the practical formation problem with  $\|a^{(6)}\| = 4.24$ , while  $\epsilon = 0.99 < 1$ . Note that the controller with the uniform gain had  $\|a\| = \sqrt{|\mathbb{E}|} \cdot 12.47 = 27.8838$ , so the iterative scheme beats it by a factor of 7 in terms of energy.

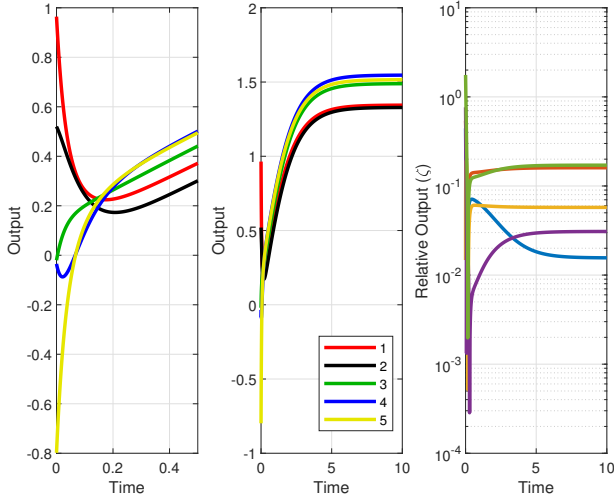


Fig. 7. The Closed-Loop with Uniform Gain  $\alpha = 9.33$ . The two leftmost graphs plot the agents' trajectories over 0.5 seconds and over 10 seconds. The rightmost graphs plots the relative outputs.

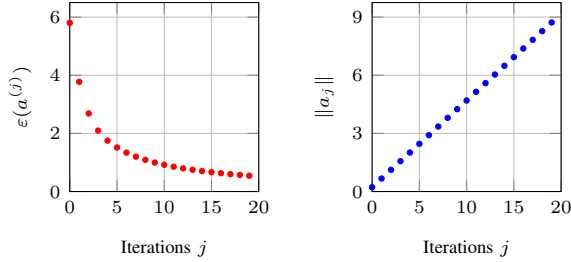


Fig. 8. The resulting  $\varepsilon$  and the norm of the gain vector  $\|a^{(j)}\|$  over iterations  $j$  when applying the iterative multi-gain control strategy to the case study of velocity coordination in vehicles.

### B. Clustering in Neural Networks

Consider a collection of  $n = 40$  neurons, each modeled by the dynamical system

$$\begin{cases} \dot{x}_i = -\frac{1}{\tau_i}x_i + b_i u_i + w_i \\ y_i = \tanh(x_i), \end{cases} \quad (7)$$

where  $x_i$  is the voltage of the  $i$ -th neuron,  $\tau_i$  is its self-correlation time,  $b_i$  is the correlation coefficient, determining the susceptibility of the neuron to external inputs, and  $w_i$  is some (constant) exogenous input. The values of the parameters  $\tau_i, b_i, w_i$  are unknown to the algorithm. However, it is known that  $\tau_i, b_i > 0$ . In the simulation, the numbers  $\tau_i$  were chosen log-uniformly between 1 and 10,  $b_i$  were log-uniformly chosen between 0.3 and 3, and  $w_i$  uniformly chosen between  $-0.5$  and  $0.5$ .

We wish to design a two-cluster formation. Namely, we divide the  $n = 40$  neurons into two groups of 20, and require that the neurons in each set will share the same steady-state output. Moreover, we require that the output of the first set will be smaller than the output of the second set by 1. We denote the desired formation by  $\zeta^*$ . We allow an error margin of  $\varepsilon = 0.2$ . We use a random Erdős-Rényi graph, where the probability of each edge to appear is  $p = 0.25$ . We choose proportional controllers  $\mu_e = \zeta_e - (\zeta^*)_e$  with gain equal to 1.

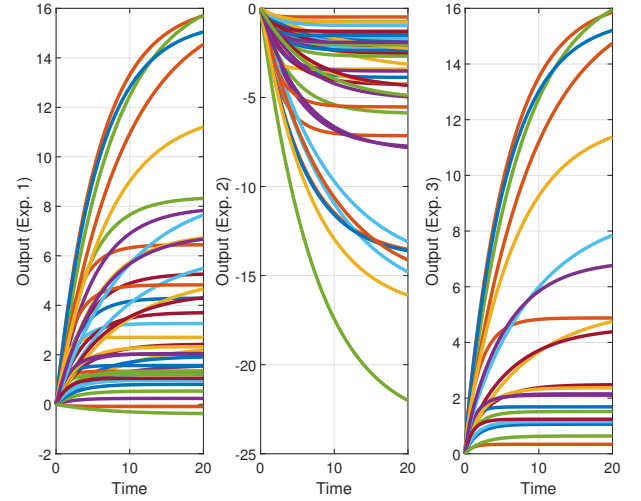


Fig. 9. Results of First Set of Experiments for the Neurons

The closed-loop generalizes the model described in the case-study of [37], achieved for  $\zeta^* = 0$ .

We apply the amplification scheme presented in Algorithm 2 and choose the desired value  $y^* = [0, \dots, 0, 1, \dots, 1]^T$ . Note that the plants are MEIP, but not output-strictly MEIP. In all cases, the first and second experiments are conducted with  $\beta_i = 0.01$ , and  $y_{\text{ref}} = \pm 100$ . Based on the results of the previous experiments, we run a third experiment on each of the agents for which this is required, this time with  $\beta_i = 1$  and  $y_{\text{ref}} = \pm 2$ , where the sign is chosen according to Algorithm 1. The experimental results of the plants are available in Figure 9.

We now estimate each  $m_i$  for  $i = 1, \dots, 40$  using Remark 4, and achieve  $m = 61.1740$ . As for estimating  $M$ , we have  $\Gamma_e(\zeta_e) = \zeta_e^2$ , so  $\Gamma(\zeta) = \|\zeta\|^2$ . The minimum is at  $x_0 = 0$ , and by definition we have  $M = \min_{x \in \text{Im}(\mathcal{E}^T): \|x - x_0\| = \varepsilon} \Gamma(x) = |\mathbb{E}| \varepsilon^2$ . Thus, we get  $\alpha = \frac{m}{M} = \frac{m}{|\mathbb{E}| \varepsilon^2} = 8.8402$ . To verify the algorithm, we run the closed-loop system  $(\mathcal{G}, \Sigma, \Pi, \alpha \mathbb{1})$  with the gain  $\alpha$  we found. The results are available in Figure 10. One can see that the overall control goal is achieved - the agents converge to a steady-state which is  $\varepsilon$ -close to the desired formation. However, as before, the agents actually converge to a much closer steady-state than predicted by the algorithm.

Applying the simplified multi-gain scheme, we start with  $a^{(0)} = \mathbb{1}_{|\mathbb{E}|}$ , we choose the step size  $h = 1$  and apply Algorithm 3. In fact, since we consider again a proportional controller, we receive  $v = \mathbb{1}_{|\mathbb{E}|}$ . The corresponding norm of the gain vector and the resulting  $\varepsilon$  in each iteration is illustrated in Fig. 11. After 4 iterations, we already arrive at a vector, which solves the specified practical formation problem with  $\|a^{(4)}\| = 65.76$ , while  $\varepsilon = 0.19 < 0.2$ . Note that the controller with the uniform gain had  $\|a\| = \sqrt{|\mathbb{E}|} \cdot 8.8402 = 116.2747$ , so the iterative scheme beats it by a factor of 2 in terms of energy.

## VII. CONCLUSIONS AND FUTURE WORK

We presented an approach for model-free practical cooperative control for diffusively coupled systems only on the

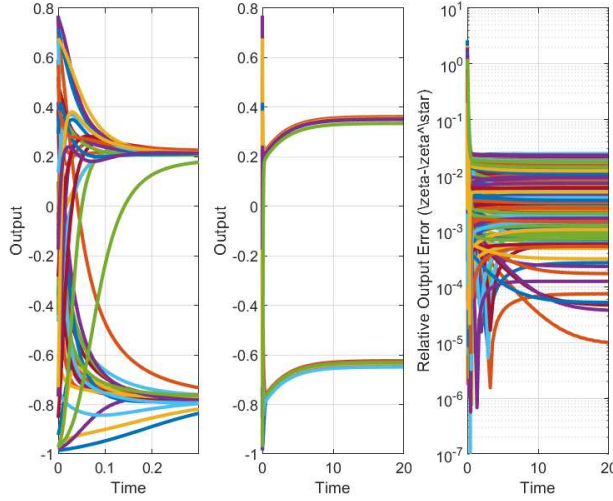


Fig. 10. The Closed-Loop with Uniform Gain  $\alpha = 8.8402$ . The two leftmost graphs plot the agents' trajectories over 0.3 seconds and over 20 seconds. The rightmost graph plots the error  $\zeta(t) - \zeta^*$ .

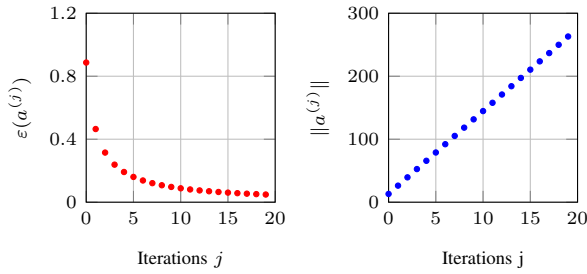


Fig. 11. The resulting  $\varepsilon$  and the norm of the gain vector  $\|a^{(j)}\|$  over iterations  $j$  when applying the iterative multi-gain control strategy to the case study of neural network clustering.

premise of passivity of the agents. The presented approach led to two control schemes: with additional two or three experiments on the agents, we can upper bound the controller gain which solves the practical formation problem, or we can iteratively adapt the adjustable gain vector until practical formation is reached. Both approaches are especially simple in their application, while still being scalable and providing theoretical guarantees.

Future research might try and improve the presented methods, either by reducing the number of experiments needed on each agent, or by achieving faster practical convergence using iterations. One might also try to use very limited knowledge on the agents to achieve the said improvement. Other possible directions include introducing data-driven solutions to more intricate problems using the network optimization framework, e.g. fault detection and isolation.

## REFERENCES

- [1] N. Chopra and M. Spong, *Advances in Robot Control, From Everyday Physics to Human-Like Movements*, ch. Passivity-based Control of Multi-Agent Systems, pp. 107–134. Springer, 2006.
- [2] A. Franchi, P. R. Giordano, C. Secchi, H. I. Son, and H. H. Bulthoff, “Passivity-based decentralized approach for the bilateral teleoperation of a group of uavs with switching topology,” in *IEEE International Conference on Robotics and Automation*, (Piscataway, NJ, USA), pp. 898–905, 2011.
- [3] L. Scardovi, M. Arcak, and E. D. Sontag, “Synchronization of interconnected systems with an input-output approach. part ii: State-space result and application to biochemical networks,” in *Proceedings of the 48th IEEE Conference on Decision and Control (CDC) held jointly with 2009 28th Chinese Control Conference*, pp. 615–620, Dec 2009.
- [4] L. Scardovi, M. Arcak, and E. D. Sontag, “Synchronization of interconnected systems with applications to biochemical networks: An input-output approach,” *IEEE Transactions on Automatic Control*, vol. 55, no. 6, pp. 1367–1379, 2010.
- [5] M. Bando, K. Hasebe, A. Nakayama, A. Shibata, and Y. Sugiyama, “Dynamical model of traffic congestion and numerical simulation,” *Phys. Rev. E*, vol. 51, pp. 1035–1042, Feb 1995.
- [6] A. Fujita, J. R. Sato, H. M. Garay-Malpartida, R. Yamaguchi, S. Miyano, M. C. Sogayar, and C. E. Ferreira, “Modeling gene expression regulatory networks with the sparse vector autoregressive model,” *BMC Systems Biology*, vol. 1, p. 39, Aug 2007.
- [7] A. Julius, M. Zavlanos, S. Boyd, and G. J. Pappas, “Genetic network identification using convex programming,” *IET Systems Biology*, vol. 3, pp. 155–166, May 2009.
- [8] S. Boccaletti, M. Ivanchenko, V. Latora, A. Pluchino, and A. Rapisarda, “Detecting complex network modularity by dynamical clustering,” *Phys. Rev. E*, vol. 75, 2007.
- [9] D. Urban and T. Keitt, “Landscape connectivity: A graph-theoretic perspective,” *Ecology*, vol. 82, no. 5, pp. 1205–1218, 2001.
- [10] P. Monestiez, J.-S. Bailly, P. Lagacherie, and M. Voltz, “Geostatistical modelling of spatial processes on directed trees: Application to fluvial extent,” *Geoderma*, vol. 128, no. 3, pp. 179 – 191, 2005. Pedometrics 2003.
- [11] E. Zheleva, E. Terzi, and L. Getoor, “Privacy in social networks,” *Synthesis Lectures on Data Mining and Knowledge Discovery*, vol. 3, no. 1, pp. 1–85, 2012.
- [12] J. Sabater and C. Sierra, “Reputation and social network analysis in multi-agent systems,” in *Proceedings of the First International Joint Conference on Autonomous Agents and Multiagent Systems: Part 1, AAMAS '02*, pp. 475–482, ACM, 2002.
- [13] M. J. Naylor, L. C. Rose, and B. J. Moyle, “Topology of foreign exchange markets using hierarchical structure methods,” *Physica A: Statistical Mechanics and its Applications*, vol. 382, no. 1, pp. 199–208, 2007. Applications of Physics in Financial Analysis.
- [14] D. Materassi and G. Innocenti, “Unveiling the connectivity structure of financial networks via high-frequency analysis,” *Physica A: Statistical Mechanics and its Applications*, vol. 388, no. 18, pp. 3866–3878, 2009.
- [15] Z.-S. Hou and Z. Wang, “From model-based control to data-driven control: Survey, classification and perspective,” *Inf. Sci.*, vol. 235, pp. 3–35, June 2013.
- [16] P. Tabuada, W. Ma, J. Grizzle, and A. D. Ames, “Data-driven control for feedback linearizable single-input systems,” in *2017 IEEE 56th Annual Conference on Decision and Control (CDC)*, pp. 6265–6270, Dec 2017.
- [17] X. Bu, Z. Hou, and H. Zhang, “Data-driven multiagent systems consensus tracking using model free adaptive control,” *IEEE Transactions on Neural Networks and Learning Systems*, vol. 29, pp. 1514–1524, May 2018.
- [18] H. Jiang and H. He, “Data-driven distributed output consensus control for partially observable multiagent systems,” *IEEE Transactions on Cybernetics*, pp. 1–11, 2018.
- [19] F. Bianchini, G. Fenu, G. Giordano, and F. A. Pellegrino, “Model-free tuning of plants with parasitic dynamics,” in *2017 IEEE 56th Annual Conference on Decision and Control (CDC)*, pp. 499–504, Dec 2017.
- [20] D. D. Šiljak, “Decentralized control and computations: Status and prospects,” *A. Rev. Control*, vol. 20, 1996.
- [21] Y. Zheng, S. E. Li, K. Li, and W. Ren, “Platooning of connected vehicles with undirected topologies: Robustness analysis and distributed H-infinity controller synthesis,” *IEEE Transactions on Intelligent Transportation Systems*, vol. 19, pp. 1353–1364, 2018.
- [22] W. Yu, P. DeLellis, G. Chen, M. di Bernardo, and J. Kurths, “Distributed adaptive control of synchronization in complex networks,” *IEEE Transactions on Automatic Control*, vol. 57, pp. 2153–2158, 2012.
- [23] J. M. Montenbruck and F. Allgöwer, “Some problems arising in controller design from big data via input-output methods,” in *2016 IEEE 55th Annual Conference on Decision and Control (CDC)*, pp. 6525–6530, 2016.

- [24] A. Romer, J. M. Montenbruck, and F. Allgöwer, “Sampling strategies for data-driven inference of passivity properties,” in *2017 IEEE 56th Annual Conference on Decision and Control (CDC)*, pp. 6389–6394, 2017.
- [25] M. Tanemura and S.-i. Azuma, “Efficient data-driven estimation of passivity properties,” *IEEE Control Systems Letters*, vol. 3, pp. 398–403, 2019.
- [26] A. Romer, J. Berberich, J. Köhler, and F. Allgöwer, “One-shot verification of dissipativity properties from input-output data,” *IEEE Control Systems Letters*, vol. 3, pp. 709–714, 2019.
- [27] C. A. Desoer and M. Vidyasagar, *Feedback Systems: Input-Output Properties*. SIAM, 1975.
- [28] H. K. Khalil, *Nonlinear Systems*. Pearson, 3rd ed., 2001.
- [29] M. Arcak, “Passivity as a design tool for group coordination,” *IEEE Transactions on Automatic Control*, vol. 52, pp. 1380–1390, Aug. 2007.
- [30] H. Bai, M. Arcak, and J. Wen, *Cooperative Control Design: A Systematic, Passivity-Based Approach*. Communications and Control Engineering, Springer, 2011.
- [31] A. Pavlov and L. Marconi, “Incremental passivity and output regulation,” *Systems & Control Letters*, vol. 57, no. 5, pp. 400 – 409, 2008.
- [32] G. H. Hines, M. Arcak, and A. K. Packard, “Equilibrium-independent passivity: A new definition and numerical certification,” *Automatica*, vol. 47, no. 9, pp. 1949–1956, 2011.
- [33] M. Bürger, D. Zelazo, and F. Allgöwer, “Duality and network theory in passivity-based cooperative control,” *Automatica*, vol. 50, no. 8, pp. 2051–2061, 2014.
- [34] M. Sharf and D. Zelazo, “A network optimization approach to cooperative control synthesis,” *IEEE Control Systems Letters*, vol. 1, pp. 86–91, July 2017.
- [35] M. Sharf and D. Zelazo, “Analysis and synthesis of MIMO multi-agent systems using network optimization,” *IEEE Transactions on Automatic Control*, 2018.
- [36] A. Jain, M. Sharf, and D. Zelazo, “Regulatization and feedback passivation in cooperative control of passivity-short systems: A network optimization perspective,” *IEEE Control Systems Letters*, vol. 2, pp. 731–736, 2018.
- [37] M. Sharf and D. Zelazo, “Network identification: A passivity and network optimization approach,” in *2018 IEEE 57th Annual Conference on Decision and Control (CDC)*, 2018.
- [38] A. Jain, M. Sharf, and D. Zelazo, “Passivation and Cooperative Control of Equilibrium-Independent Passivity-Short Systems,” *arXiv e-prints*, p. arXiv:1901.06512, 2019.
- [39] J. M. Montenbruck, M. Bürger, and F. Allgöwer, “Practical synchronization with diffusive couplings,” *Automatica*, vol. 53, pp. 235 – 243, 2015.
- [40] J. Kim, J. Yang, H. Shim, J. Kim, and J. H. Seo, “Robustness of synchronization of heterogeneous agents by strong coupling and a large number of agents,” *IEEE Transactions on Automatic Control*, vol. 61, no. 10, pp. 3096–3102, 2016.
- [41] C. Godsil and G. Royle, *Algebraic Graph Theory*. Graduate Texts in Mathematics, Springer New York, 2001.
- [42] R. T. Rockafellar, *Convex Analysis*. Princeton Landmarks in Mathematics and Physics, Princeton University Press, 1997.
- [43] K.-K. Oh, M.-C. Park, and H.-S. Ahn, “A survey of multi-agent formation control,” *Automatica*, vol. 53, pp. 424 – 440, 2015.
- [44] A. Romer, J. M. Montenbruck, and F. Allgöwer, “Determining dissipation inequalities from input-output samples,” in *Proc. 20th IFAC World Congress*, pp. 7789–7794, 2017.
- [45] D. A. Bristow, M. Tharayil, and A. G. Alleyne, “A survey of iterative learning control,” *IEEE Control Systems Magazine*, vol. 26, no. 3, pp. 96–114, 2006.
- [46] J. Feiling, A. Zeller, and C. Ebenbauer, “Derivative-free optimization algorithms basen on non-commutative maps,” *IEEE Control Systems Letters*, vol. 2, pp. 743–748, 2018.

## APPENDIX

The purpose of this appendix is to give a full proof of Proposition 1 and Theorem 3.

### A. Proving Proposition 1

In order to prove the proposition, we use the notion of cursive relations established in [38]:

**Definition 4** (Cursive Relations, [38]). *A set  $A \subset \mathbb{R}^2$  is called cursive if there exists a curve  $\alpha : \mathbb{R} \rightarrow \mathbb{R}^2$  such that the following conditions hold:*

- i) *The set  $A$  is the image of  $\alpha$ .*
- ii) *The map  $\alpha$  is continuous.*
- iii) *The map  $\alpha$  satisfies  $\lim_{|t| \rightarrow \infty} \|\alpha(t)\| = \infty$ .*
- iv) *The set  $\{t \in \mathbb{R} : \exists s \neq t, \alpha(s) = \alpha(t)\}$  has measure zero.*

*A relation  $\mathcal{Y}$  is called cursive if the set  $\{(p, q) : q \in \mathcal{Y}(p)\}$  is cursive.*

The notion of cursive relations is useful as they can help prove that systems are MEIP. Specifically,

**Theorem 4.** *A monotone cursive relation is maximally monotone.*

The reader is referred to [38] for a proof. We can now prove Proposition 1:

*Proof.* Consider an arbitrary steady-state of the system. As  $h$  is continuous and strictly monotone ascending, hence invertible, we must have  $\dot{x} = 0$  for any steady-state input-output pair. Thus, we conclude that any steady-state input-output pair can be written as  $(f(\sigma)/g(\sigma), h(\sigma))$  for some  $\sigma \in \mathbb{R}$ . We first show passivity with respect to every steady-state, and then show that the steady-state input-output relation is maximally monotone. Take a steady-state  $(f(x_0)/g(x_0), h(x_0))$  of the system, and define  $S(x) = \int_{x_0}^x \frac{h(\sigma) - h(x_0)}{g(\sigma)} d\sigma$ . We claim that  $S$  is a storage function for the steady-state input-output pair  $(f(x_0)/g(x_0), h(x_0))$ . Indeed,  $S(x) \geq 0$ , with equality only at  $x_0$ , immediately follows from strict monotonicity of  $h$  and the positivity of  $g$ . As for the inequality defining passivity, we have:

$$\begin{aligned} \frac{d}{dt} S(x) &= \frac{h(x) - h(x_0)}{g(x)} (-f(x) + g(x)u) = \\ &= (h(x) - h(x_0))u - \frac{f(x)}{g(x)} (h(x) - h(x_0)) = \\ &= (h(x) - h(x_0)) \left( u - \frac{f(x_0)}{g(x_0)} \right) - \left( \frac{f(x)}{g(x)} - \frac{f(x_0)}{g(x_0)} \right) (h(x) - h(x_0)), \end{aligned}$$

where the second term is negative as  $\frac{f}{g}, h$  are strictly monotone ascending, and the first term is  $(y - h(x_0))(u - \frac{f(x_0)}{g(x_0)})$ . This proves that the system is indeed passive with respect to any steady-state input-output pair. As for maximal monotonicity of the steady-state relation, we recall that it can be parameterized as  $(f(\sigma)/g(\sigma), h(\sigma))$  for  $\sigma \in \mathbb{R}$ . We claim that this relation is both monotone and cursive, which will show that the relation is maximal monotone. Monotonicity follows from the implications

$$\frac{f(x_0)}{g(x_0)} > \frac{f(x_1)}{g(x_1)} \iff x_0 > x_1 \iff h(x_0) > h(x_1), \quad \forall x_0, x_1 \quad (8)$$

due to strict monotonicity. As for cursiveness, the map  $\sigma \mapsto (f(\sigma)/g(\sigma), h(\sigma))$  is a curve whose image is the relation. Moreover, it's clear that the map is continuous, and also



injective due to (8). Lastly, we have

$$\lim_{|t| \rightarrow \infty} \left\| \left( \frac{f(t)}{g(t)}, h(t) \right) \right\| \geq \lim_{t \rightarrow \infty} \max \left\{ \left| \frac{f(t)}{g(t)} \right|, |h(t)| \right\} = \infty \quad (9)$$

proving that the steady-state relation is also cursive, and completing the proof.  $\square$

### B. Proving Theorem 3.

We first state and prove the following lemma:

**Lemma 4.** *Suppose that the assumptions of Theorem 3 hold, and let  $C > 0$  be any constant. Define  $A_1 = \{y \in \mathbb{R}^n : \|\mathcal{E}^T y - \zeta^*\| \leq C\}$  and  $A_2 = \{y \in \mathbb{R}^n : \sum_i k_i^{-1}(y_i) = 0\}$ . Then the set  $A_1 \cap A_2$  is bounded.*

*Proof.* First, we note that the inequality  $\|\mathcal{E}^T y - \zeta^*\| \leq C$  implies that for any edge  $\{i, j\} \in \mathbb{E}$ , we have  $|y_i - y_j| \leq C + \|\zeta^*\|$  by the triangle inequality. We let  $\omega = (C + \|\zeta^*\|)\text{diam}(\mathcal{G})$ , where  $\text{diam}(\mathcal{G})$  is the diameter of the graph  $\mathcal{G}$ , so that if there exists some  $i, j \in \mathbb{V}$  such that  $|y_i - y_j| > \omega$  then  $y \notin A_1$ . Moreover, let  $z = k(0)$ . Then  $\sum_i k_i^{-1}(z_i) = 0$ . Moreover, if  $y \in \mathbb{R}^n$  satisfies  $\forall i : y_i > z_i$ , then  $y \notin A_2$ . Indeed, for each  $i$  we have  $k_i^{-1}(y_i) \geq k_i^{-1}(z_i)$ , and  $k_{i_0}^{-1}(z_{i_0}) > k_{i_0}^{-1}(y_{i_0})$ , meaning that  $\sum_i k_i^{-1}(y_i) > \sum_i k_i^{-1}(z_i) = 0$ . Similarly, if  $\forall i, z_i > y_i$  then  $y \notin A_2$ . We now claim that for any  $y \in A_1 \cap A_2$  and any  $i \in \mathbb{V}$ , we have  $C_1 < y_i < C_2$ , where  $C_1 = \min_j z_j - \omega - 1$  and  $C_2 = \max_j z_j + \omega + 1$ . Indeed, take any  $y \in \mathbb{R}^n$ , and suppose there exists  $i \in \mathbb{V}$  such that  $y_i \geq C_2$ . There are two possibilities.

- There is some  $k \in \mathbb{V}$  such that  $y_k < \max_j z_j + 1$ . Then  $|y_i - y_k| > \omega$ , implying that  $y \notin A_1$ .
- For any  $k \in \mathbb{V}$ ,  $y_k \geq \max_j z_j + 1$ , implying that  $y \notin A_2$ .

Similarly, one shows that if there's some  $i$  such that  $y_i \leq C_1$ , then  $y \notin A_1 \cap A_2$ . This completes the proof.  $\square$

*Proof of Theorem 3.* Consider the solution  $y(a)$  of  $0 = k^{-1}(y) + \mathcal{E} \text{diag}(a) \gamma(\mathcal{E}^T y)$  as a function of  $a$ . Then  $y(a)$  is a differentiable function by the inverse function theorem, and it's differential is given by:

$$\frac{dy}{da} = -X(y(a)) \mathcal{E} \text{diag}(\gamma(\mathcal{E}^T y(a))), \quad (10)$$

where the matrix  $X(y)$  is given by

$$X(y) = [\text{diag}(\nabla k^{-1}(y)) + \mathcal{E} \text{diag}(\nabla \gamma(\mathcal{E}^T y)) \mathcal{E}^T]^{-1}. \quad (11)$$

We note that  $X(y)$  is a positive-definite matrix for any  $y \in \mathbb{R}^n$ , by Proposition 2 in [37]. We conclude that the gradient of  $F$  is given by:

$$\nabla F(a) = -\text{diag}(\gamma(\mathcal{E}^T y(a))) \mathcal{E}^T X(y(a)) \mathcal{E}(\mathcal{E}^T y(a) - \zeta^*). \quad (12)$$

We note that  $v^T \text{diag}(\gamma(\mathcal{E}^T y(a))) = \mathcal{E}^T y(a) - \zeta^*$ , as  $\gamma_e(x_e) = 0$  if and only if  $x_e = \zeta_e^*$  by strict monotonicity. Thus,

$$v^T \nabla F(a) = -(\mathcal{E}(\mathcal{E}^T y(a) - \zeta^*))^T X(y(a)) \mathcal{E}(\mathcal{E}^T y(a) - \zeta^*) \quad (13)$$

which is  $\leq 0$  as  $X(y(a))$  is a positive-definite matrix.

Now, we claim that  $v^T \nabla F(a) = 0$  if and only if  $\mathcal{E}^T y(a) = \zeta^*$ . Indeed,  $\zeta^* \in \text{Im}(\mathcal{E}^T)$ , so we denote  $\zeta^* = \mathcal{E}^T y_0$  for

some  $y_0$ . As  $X(y(a))$  is positive definite, (13) implies that  $v^T \nabla F(a) = 0$  if and only if  $\mathcal{E}(\mathcal{E}^T y(a) - \zeta^*) = \mathcal{E} \mathcal{E}^T (y(a) - y_0)$  is the zero vector. The kernel of the Laplacian  $\mathcal{E} \mathcal{E}^T$  is the span of the all-one vector  $\mathbb{1}_n$ , so  $y(a) - y_0 = \kappa \mathbb{1}_n$  for some  $\kappa > 0$ , hence  $\mathcal{E}^T y(a) = \mathcal{E}^T y_0 = \zeta^*$ . This concludes the first part of the proof.

As for convergence, we know that if  $h$  is small enough, then  $F(a^{(j+1)}) < F(a^{(j)})$ . However, the value of  $h$  so that  $F(a^{(j+1)}) < F(a^{(j)})$  can depend on  $a^{(j)}$  itself. However, it is obvious that if  $h$  is small enough, then for any  $j$ , we have  $F(a^{(j)}) \leq F(a^{(0)})$ . We let  $C = F(a^{(0)}) = \|\mathcal{E}^T y(a^{(0)}) - \zeta^*\|$ , and consider the sets  $A_1 = \{y : \|\mathcal{E}^T y - \zeta^*\| \leq C\}$  and  $A_2 = \{y : \sum_i k_i^{-1}(y_i) = 0\}$ .

For any  $j$ , we know that  $y(a^{(j)}) \in A_1$  by above, and that  $y(a^{(j)}) \in A_2$  by the steady-state equation  $0 = k^{-1}(y(a)) + \mathcal{E} \text{diag}(a) \gamma(\mathcal{E}^T y(a))$ . This shows that all steady-state outputs achieved during the algorithm are in the set  $\mathcal{D} = A_1 \cap A_2$ , which is bounded by Lemma 4. The mapping sending a matrix to its minimal singular value is continuous, meaning that  $\sigma(X(y))$  achieves a minimum on the set  $\mathcal{D}$  at some point  $y_1$ , and the minimum is positive as  $X(y_1)$  is positive-definite. We denote the minimum value by  $\underline{\sigma}(\mathcal{D})$ .

Now, consider equation (13). We get that  $v^T \nabla F(a)$  is bounded by above  $-\underline{\sigma}(\mathcal{D}) \|\mathcal{E}(\mathcal{E}^T y(a) - \zeta^*)\|^2$ . In turn, we saw above that unless  $\mathcal{E}^T y(a) = \zeta^*$ ,  $\mathcal{E}(\mathcal{E}^T y(a) - \zeta^*) \neq 0$ , meaning that  $\|\mathcal{E}(\mathcal{E}^T y(a) - \zeta^*)\| \geq \varsigma \|\mathcal{E}^T y(a) - \zeta^*\|^2$ , where  $\varsigma$  is the minimal nonzero singular value of  $\mathcal{E}$ . Hence, at any time step  $j$ ,  $v^T \nabla F(a^{(j)}) < -\underline{\sigma}(\mathcal{D}) \varsigma F(a^{(j)})$ . In turn we conclude that  $F(a^{(j+1)}) = F(a^{(j)}) - h \underline{\sigma}(\mathcal{D}) \varsigma F(a^{(j)}) + \mathcal{O}(h) = (1 - h \underline{\sigma}(\mathcal{D}) \varsigma) F(a^{(j)}) + \mathcal{O}(h)$ . Iterating this equation shows that eventually,  $F(a^{(j)}) < \varepsilon$ , completing the proof.  $\square$